



Review

Nanomaterials with Excellent Adsorption Characteristics for Sample Pretreatment: A Review

Wen-Xin Liu ^{1,2}, Shuang Song ¹ , Ming-Li Ye ², Yan Zhu ³, Yong-Gang Zhao ^{2,*} and Yin Lu ^{2,*}

¹ College of Environment, Zhejiang University of Technology, Hangzhou 310014, China; lwx187221@163.com (W.-X.L.); ss@zjut.edu.cn (S.S.)

² College of Biological and Environmental Engineering, Zhejiang Shuren University, Hangzhou 310015, China; yemingli@zjsru.edu.cn

³ Department of Chemistry, Zhejiang University, Hangzhou 310027, China; zhuyan@zju.edu.cn

* Correspondence: zhyg91213@163.com (Y.-G.Z.); luyin@zjsru.edu.cn (Y.L.)

Abstract: Sample pretreatment in analytical chemistry is critical, and the selection of materials for sample pretreatment is a key factor for high enrichment ability, good practicality, and satisfactory recoveries. In this review, the recent progress of the sample pretreatment methods based on various nanomaterials (i.e., carbon nanomaterials, porous nanomaterials, and magnetic nanomaterials) with excellent adsorption efficiency, selectivity, and reproducibility, as well as their applications, are presented. Due to the unique nanoscale physical–chemical properties, magnetic nanomaterials have been used for the extraction of target analytes by easy-to-handle magnetic separation under a magnetic field, which can avoid cumbersome centrifugation and filtration steps. This review also highlights the preparation process and reaction mechanism of nanomaterials used in the sample pretreatment methods, which have been applied for the extraction organophosphorus pesticides, fluoroquinolone antibiotics, phenoxy carboxylic acids, tetracycline antibiotics, hazardous metal ions, and rosmarinic acid. In addition, the remaining challenges and future directions for nanomaterials used as sorbents in the sample pretreatment are discussed.

Keywords: carbon nanomaterial; porous nanomaterials; magnetic nanomaterials; sample pretreatment; solid phase extraction



Citation: Liu, W.-X.; Song, S.; Ye, M.-L.; Zhu, Y.; Zhao, Y.-G.; Lu, Y.

Nanomaterials with Excellent Adsorption Characteristics for Sample Pretreatment: A Review.

Nanomaterials **2022**, *12*, 1845.

<https://doi.org/10.3390/nano12111845>

nano12111845

Academic Editor: Giorgio Vilardi

Received: 30 April 2022

Accepted: 25 May 2022

Published: 27 May 2022

Publisher's Note: MDPI stays neutral with regard to jurisdictional claims in published maps and institutional affiliations.



Copyright: © 2022 by the authors. Licensee MDPI, Basel, Switzerland. This article is an open access article distributed under the terms and conditions of the Creative Commons Attribution (CC BY) license (<https://creativecommons.org/licenses/by/4.0/>).

1. Introduction

In analytical chemistry, the sample pretreatment methods are very important because they play a vital role in the whole analytical system. The complete sample analysis includes five steps: sample collection, sample pretreatment, instrumental analysis, data processing, and reporting results. The most time-consuming of these five steps is sample pretreatment, which accounts for about 60% of the whole process [1–3]. At present, solid phase extraction (SPE), with higher adsorption rate and better reproducibility, is widely used in the preconcentration of low concentration substances and the purification of complex samples [4]. As well as the SPE methods, various efficient and environmentally friendly pretreatment methods based on SPE, including solid phase microextraction (SPME), dispersed solid phase extraction (dSPE), magnetic solid-phase extraction (MSPE), the QuEChERS (quick, easy, cheap, effective, rugged, and safe) method [5–8], and the PRiME (process, robustness, improvements, matrix effects, and ease of use) pass-through cleanup procedure [9–12], have been developed. In these sample pretreatment methods, adsorbent with uniform particle size distribution, good dispersion, and high-efficiency adsorption capacity is the key factor for the performance of sample pretreatment.

With the continuous study of nanomaterials, researchers have found that nanomaterials have great potential in the field of sample pretreatment. The typical particle size range of nanomaterials is between 1~100 nm [13]; however, it does not mean that only the particle size between 1~100 nm is called nanomaterial, as long as there is a dimension within this

range, then this kind of material belongs to nanomaterial. Nanomaterials are ideal solid phase adsorption materials [14,15]. Compared with general adsorbents, nanomaterials have the following characteristics: (1) smaller particle size and larger specific surface area, which increases the interaction between particles and analytes, thus improving the ability of nanomaterials to adsorb and separate analytes [16,17]; (2) very high surface energy and diffusivity, the nanoparticles can be in full contact with each other, the adsorption equilibrium can be achieved in a short time, and the nanomaterials have unique adsorption properties for metal ions and organic pollutants [18–21]; and (3) easy to be functionalized, and specific functional groups can be introduced to achieve efficient and selective extraction of target compounds. Due to so many excellent properties, nanomaterials have been used as adsorbents in various branches of analytical chemistry [22,23], such as drug analysis, biomedicine, environmental protection and forensic medicine. It is used for qualitative and quantitative analysis of various analytes in complex samples [24,25]. For example, polymer nanomaterials have been used to analyze benzene series, p-hydroxybenzoate, and imidazolone in soil and sediment samples. The metal and mixed oxide nanomaterials [26–28], carbon-based nanomaterials [29–32], and magnetic nanomaterials [33–35] have been used to analyze substances in environmental water samples.

Nanomaterials can be divided into organic nanomaterials, inorganic nanomaterials, and organic–inorganic hybrid nanomaterials according to their composition [36]. In recent years, there is increasing research on hybrid composites, especially the magnetic hybrid composites. Magnetic nanoparticles have the characteristics of superparamagnetism, high adsorption capacity, a large specific surface area, and so on [37,38]. These characteristics make it more suitable to be adsorbent for SPE. Magnetic nanoparticles can be separated quickly by a magnetic field due to the superparamagnetism; therefore, when the analyte interacts with the magnetic nanoparticles, it can be easily separated from the complex samples by magnetic separation.

Recently, prominent progress has been obtained in nanomaterials research. In this article, we review the recent advances in the nanomaterials and discuss their classification and preparation, as well as strategies to improve their adsorption efficiency, selectivity, reproducibility, and applications in sample pretreatment. We will also pay considerable attention to the recent development in the sample pretreatment methods, with a focus on nanomaterials. Based on the applications of nanomaterials for the extraction of various chemicals (i.e., organophosphorus pesticides, phenoxy carboxylic acids, hazardous metal ions, etc.), we also provide some perspectives on the future trends of nanomaterials for the further design of novel sample pretreatment methods and beyond.

2. Synthesis of Nanomaterials and Their Applications in Sample Pretreatment

2.1. Carbon Nanomaterials

Carbon nanomaterials have always been the focus of research, because carbon nanomaterials have good adsorption, electrochemical, catalytic, and gas storage properties. Due to the different bonding modes between carbon atoms, the structure and properties of carbon nanomaterials are different. Carbon nanomaterials can be divided into the following three basic types: zero-dimensional nanoparticle clusters, such as fullerenes (C_{60}), successfully prepared by Kroto and co-workers in 1985 [39]; one-dimensional carbon nanotubes and carbon nanofibers, such as carbon nanotubes, which were discovered by Iijima in 1991 [40]; two-dimensional carbon nanolayers or membrane materials, such as graphene, which was discovered by Novoselov and co-workers [41]. With the continuous discovery of carbon nanostructures, and all of them showing very good adsorption properties and outstanding mechanical properties, researchers have a strong interest in them [42–44].

2.1.1. Application of Fullerene in Sample Pretreatment

Fullerene is a hollow particle cluster composed of carbon atoms, which is very similar to graphene in structure. Graphene is composed of six-membered rings, whereas fullerene contains not only six-membered rings, but also five-membered rings, or even

seven-membered rings [45]. Due to the different number of atoms that make up the particle group, fullerene has many isomers, but the most stable one is C_{60} ; therefore, C_{60} is the most common and widely studied and applied. As with a football, the molecular structure of C_{60} is also a spherical structure composed of thirty-two faces, of which twenty, six-membered rings, and twelve, five-membered rings, are connected by sixty carbon atoms; therefore, C_{60} is also called the football alkene [45,46].

In 2007, a stationary phase of C_{60} fullerene combined with silica for SPE was prepared by Rainer and co-workers [47]. The preparation method was probably an adsorption material prepared by linking silica and C_{60} through covalent bonds with aminopropyl as a linking agent. The C_{60} -fullerene silica had a strong retention ability for small molecules and hydrophilic molecules; therefore, the new material has a high adsorption capacity for proteins and phosphopeptides. In addition, C_{60} -fullerene silica was also used for the extraction of flavonoids, and the results showed that the recovery rate of flavonoids by C_{60} -fullerene silica SPE was 99%.

In 2019, a new type of fullerene (C_{60}), a soluble eggshell membrane protein (SESMP) composite, was prepared by Alheety and co-authors [48]. The Fe_3O_4 -NPs was grafted onto SESMP to prepare a SPE packing for arsenic in six kinds of crude oil and environmental water samples (Figure 1). Under the optimized conditions, the limit of detections of As (III) and As (V) were 0.0473 ng/mL and 0.0325 ng/mL, respectively, and the relative standard deviation (RSD) of As (III) and As (V) are 1.15% and 1.31%. The results showed that the SESMP grafted with Fe_3O_4 NPs had a good extraction of arsenic in crude oil and environmental water samples.

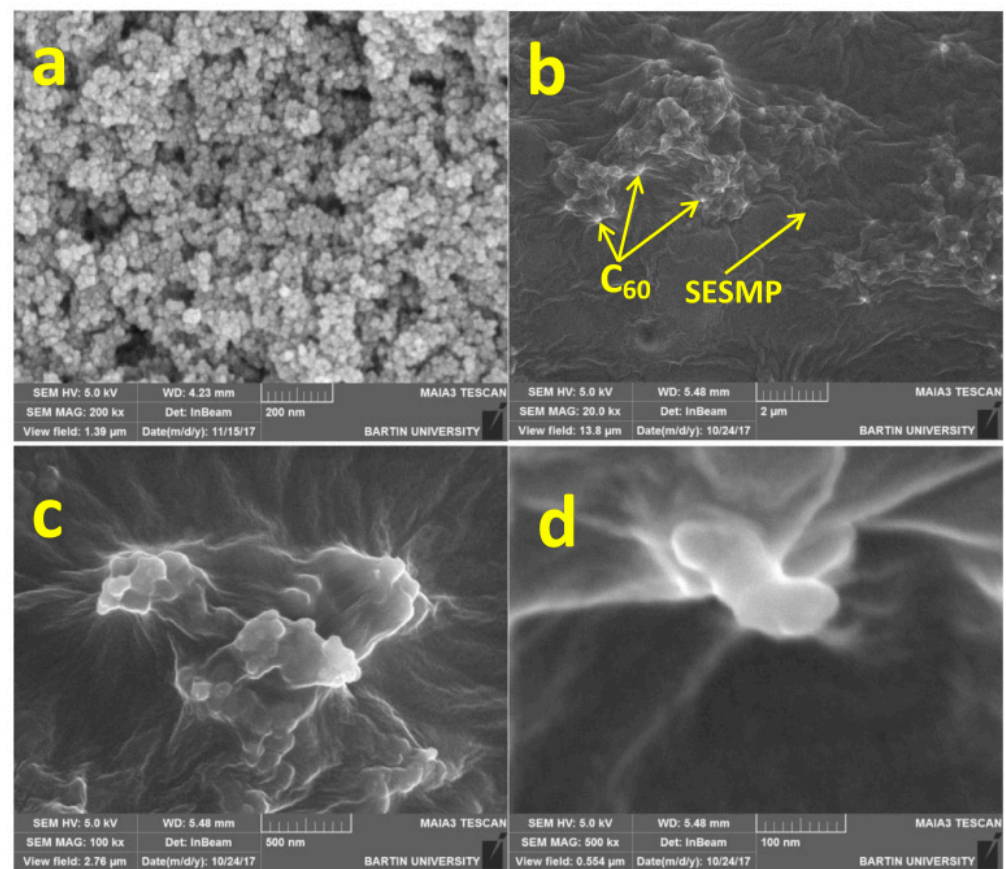


Figure 1. SEM of (a) Fe_3O_4 -NPs, (b) C_{60} -SESMP nanocomposite 2 μ m, (c) C_{60} -SESMP nanocomposite 500 nm, and (d) C_{60} -SESMP nanocomposite 100 nm. Reprinted with permission from Ref. [48]. Copyright (2019) Elsevier.

2.1.2. Synthesis of Carbon Nanotubes and Its Application in Sample Pretreatment

A carbon nanotube is a kind of quasi-one-dimensional tubular macromolecule with a helical period and hollow cavity structure, and its surface mainly shows a hexagonal network structure, which is also mixed with pentagons or heptagons. The carbon nanotubes can be seen as coiled from a hexagonal network of graphite sheets [49]. According to the number of graphite layers, it can be divided into single-walled carbon nanotubes (SWCNTs) and multi-walled carbon nanotubes (MWCNTs). Carbon nanotubes have high thermal capacity, high chemical stability, a large specific surface area, small pore size, and easy modification. It has better adsorption properties compared with traditional adsorbents; therefore, carbon nanotubes are often used as adsorbents in sample pretreatment. However, carbon nanotubes cannot selectively adsorb the target, it is necessary to functionalize carbon nanotubes to improve their selectivity. There are three main methods for the preparation of carbon nanotubes: arc discharge, laser ablation, and chemical vapor deposition (CVD).

(1) The arc square method was born in 1991. During the arc synthesis of graphite by arc method under a high resolution transmission electron microscope, MWCNTs were found for the first time [40]. Arc discharge is the most traditional method for the preparation of carbon nanotubes. Its basic principle is that under certain conditions, a large number of electrons are produced under the field electron emission effect and hot electron emission effect between the cathode and anode, which bombard the anode. The temperature of the anode increases and causes the anode to evaporate. These evaporated carbon atoms are quickly reorganized in the process of cooling to form carbon nanotubes. Although the equipment used by arc discharge method is complex, and the process parameters are difficult to control, the carbon nanotubes prepared by this method have the advantages of few structural defects, good flexibility, straight tube, high crystallinity, and so on [50–54].

(2) In 1995, Smalley team [55] successfully demonstrated the preparation of carbon nanotubes by laser ablation for the first time. Its principle and mechanisms are similar to arc discharge. Their difference lies in the different methods of making carbon atoms evaporate. Arc discharge makes anode carbon atoms evaporate by releasing a large number of electrons that bombard the anode, whereas the law of laser ablation is to vaporize carbon atoms by bombarding graphite particles containing catalysts with high-energy laser beams, then reassembling them to form carbon nanotubes, and finally depositing them on the collector with the airflow [56].

(3) The above two methods are mainly used in the laboratory, and the large-scale production of carbon nanotubes is mainly through CVD. The principle of CVD is that hydrocarbons are pyrolyzed into hydrogen and carbon atoms under the action of transition metal catalysts at appropriate ambient temperature, and then these carbon atoms are reassembled to form carbon nanotubes; however, there are two situations in the growth process of carbon nanotubes: (i) there are metal particles at the tip of carbon nanotubes; (ii) there are metal particles at the roots of carbon nanotubes. The reason for the different grounding position of metal particles is due to the different intensity of metal-carrier interaction. When the metal-carrier interaction is strong, metal particles will appear at the root of carbon nanotubes; when the metal-carrier interaction is weak, metal particles will appear at the tip of carbon nanotubes. The overall performance of carbon nanotubes prepared by this method is not as good as that of carbon nanotubes prepared by the arc discharge method and laser ablation method, but a single yield of the arc discharge method and laser ablation method is lower than that of the CVD method; therefore, CVD is widely used in the industrial production of carbon nanotubes [57–59].

In 2017, Feist and co-workers [60] developed a simple and effective method for the determination of lead, cadmium, zinc, manganese, and iron in white rice and wild rice samples by using oxidized MWCNTs as adsorbents. The limit of detection was between 0.13 ng/mL and 0.35 ng/mL. The new preconcentration method was successfully applied to food analysis with an accuracy of less than 7%. This method can be applied to the preconcentration of Pb (II), Cd (II), Zn (II), Mn (II), and Fe (III) ions in rice samples.

In 2018, Khamirchi et al. [61] reported novel MWCNTs modified by [2-(5-Bromo-2-pyridylazo)-5-(diethylamino)phenol] (Br-PADAP) for the preconcentration of a uranium ion. The result showed that the Br-PADAP-modified MWCNTs had much higher adsorption capacity for uranium ion than the original carbon nanotubes; therefore, the multi-walled MWCNT carbon nanotubes, modified by Br-PADAP, can be used as a SPE adsorbent for efficient adsorption of uranium in water treatment. Moreover, the enrichment factor of the prepared SPE column for the analysis of trace uranium in different environments was 300 times, and the interference of other ions to the pre-enrichment of uranium was minimal. The limit of detection was 0.14 µg/L and the RSD was about 3.3%.

2.1.3. Synthesis of Graphene and Its Application in Pretreatment

In the 20th century, the theory of “two-dimensional crystal structure can not exist because of its thermodynamic instability” was not overturned until Geim and others successfully prepared graphene by mechanical exfoliation. Graphene is formed by the close accumulation of carbon atoms, showing a honeycomb lattice structure, which is a two-dimensional crystal structure [62]. Both fullerenes and carbon nanotubes can be made by wrapping or crimping graphene. At present, graphene has become one of the most widely used carbon materials. Due to its special structure, graphene has good chemical stability, good mechanical strength, and a high specific surface area. Moreover, graphene also has outstanding corrosion resistance and flexibility [63,64]; therefore, graphene is more suitable for the preparation of adsorbents than carbon nanotubes and fullerenes, especially for graphene oxide (GO), because there are oxygen-containing functional groups on GO, such as –OH, –COOH, C–O–C. Moreover, the application of GO to the preparation of composites will make the prepared composites have a better adsorption efficiency and faster adsorption kinetics [65,66]. Graphene shows a great application prospect in pre-enrichment, and has become one of the most widely used carbon nanomaterials in sample pretreatment. The preparation of graphene is mainly divided into physical methods and chemical methods. Mechanical stripping is the most traditional method in terms of physical methods, and CVD is the most widely used method in terms of chemical methods.

(1) The mechanical stripping method is to remove graphene from graphite by tape or ultrasonic dispersion. In 2004, graphene stripped from graphite using adhesive tape was done for the first time by Novoselov and co-workers [41]. The tape with graphene, and the silicon wafer coated with silicon dioxide film, were put into the solution to adsorb some thin graphene sheets on the silicon wafer by van der Waals force, so as to achieve the purpose of separating the graphene layer. The process of mechanical stripping is simple, and the graphene prepared by mechanical stripping has few structural defects, but its yield is low, and the uniformity cannot be accurately controlled.

(2) The principle of preparing graphene by CVD is that the carbon-containing compounds are decomposed into carbon atoms at a high temperature, and then these separated carbon atoms are deposited on the surface of the matrix to obtain graphene. In 2006, Somani and co-workers [67] separated carbon atoms by putting camphor in the ambient atmosphere of Ar, baking it at 180 °C, and finally depositing it on the surface of metal Ni to get graphene. CVD has the potential to be produced on a large scale. Moreover, the graphene prepared by this method can maintain good uniformity in the case of large area [68,69].

In 2021, Silvestro and co-workers [70] adjusted the hydrophilicity of chitosan-based membranes by introducing different amounts of GO in order to obtain multifunctional materials used as adsorbents in SPE. The results showed that the introduction of GO indeed reduced the hydrophilicity of the composite membrane and increased the adsorption capacity of hydrophobic pollutants.

In 2021, a novel molybdenum disulfide–GO composite (MoS₂/GO) was synthesized by Wenjing and co-workers [71], which was used as an adsorbent for dispersive SPE (Figure 2). MoS₂/GO was used for the adsorption of four preservatives (i.e., methylparaben, ethylparaben, propylparaben, and butylparaben) prior to high performance liquid chromatogra-

phy (HPLC) analysis. Under optimal conditions, the results showed that MoS₂/GO has a strong enrichment ability for these preservatives. The RSD obtained by this method was less than 8.0%, and the limit of detection was between 0.4 ng/mL and 2.3 ng/mL. It can be seen that MoS₂/GO has broad prospects in the determination of parabens preservatives.

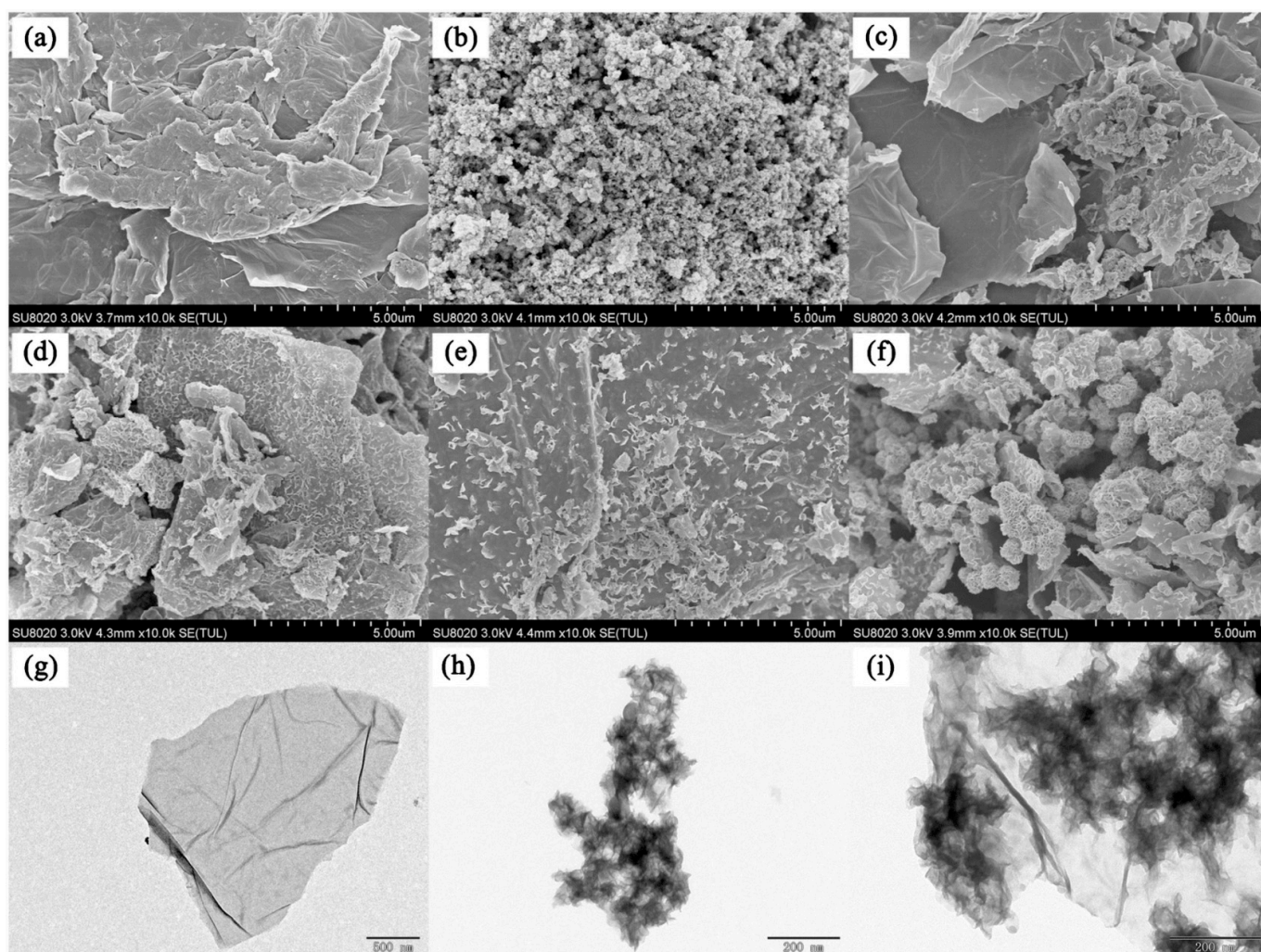


Figure 2. SEM images of GO: (a) MoS₂, (b) MoS₂/GO-0.5, (c) MoS₂/GO-1, (d) MoS₂/GO-1.5, (e) and MoS₂/GO-2. (f) TEM images of GO: (g) MoS₂ (h) and MoS₂/GO-1.5. (i). Reprinted with permission from Ref. [71]. Copyright (2021) Springer Wine.

2.2. Porous Nanomaterials

Porous materials can be divided into three categories according to the pore size: macroporous materials (pore size greater than 50 nm), mesoporous materials (pore size between 2 and 50 nm), and microporous materials (pore size less than 2 nm) [72–75]. It can also be classified according to its composition, which can be divided into inorganic porous materials, organic porous materials and inorganic–organic hybrid porous materials. Porous materials usually have the characteristics of a relatively large, specific surface area, high pore melting, easy mass transfer, and high adsorption capacity, so they are widely used in sample pretreatment [76,77].

2.2.1. Synthesis of MOF and Its Application in Sample Pretreatment

In 1995, metal-organic frameworks (MOFs) were created by Yaghi and co-authors [78]. MOF is a new type of organic–inorganic hybrid crystalline porous material with a regular pore or hole structure, which is formed by the connection between an inorganic metal and

an organic functional group through a coordination bond, hydrogen bond, π bond, and so on [79]. MOFs have the advantages of regular pore size, large adsorption capacity, high mechanical strength, wide range of morphology, and easy-to-modify properties [80,81]. Researchers can design the pore size and space layout of MOFs according to their needs, and then make specific modifications [82–86].

(1) The main preparation method of MOFs in laboratories is the solvothermal method. The principle of a solvothermal method is that inorganic salts and organic linkers are mixed, transferred to a sealed reaction container, and then heated to make the insoluble frameworks grow. Although the solvothermal method is used in the laboratory, it is not suitable for large-scale preparation, because the ratio of surface area to volume is greatly reduced by increasing the volume of the reaction vessel, which affects the nucleation effect of MOFs on the surface of reaction vessel. Moreover, the reaction time of solvothermal method is longer.

(2) Microwave-assisted solvothermal synthesis was first proposed by Ni and co-workers [87] in 2006. The study showed that microwave-assisted solvothermal synthesis has advantages of fast synthesis speed and good control of crystal size and shape, but it also has the disadvantage of not producing large crystals.

In 2020, a new type of mixed-matrix membrane (MMM) (Figure 3), based on cationic metal organic frameworks, namely, UiO-66-NMe₃⁺MMM (Figure 4), was synthesized by Wu and co-workers [88]. It was used to adsorb six kinds of phenoxy carboxylic acids (PCAs) from water prior to ultra-high performance liquid chromatography-tandem mass spectrometry (UHPLC-MS/MS) analysis. Under optimal conditions, UiO-66-NMe₃⁺MMM showed excellent adsorption efficiency on PCAs. The limit of detection could be as low as 0.03~0.59 ng/L, and the intra-day and inter-day RSD were 2.30% and 3.26%. The results showed that it could be used for the analysis of PCAs in complex water samples such as sewage and reservoir water.

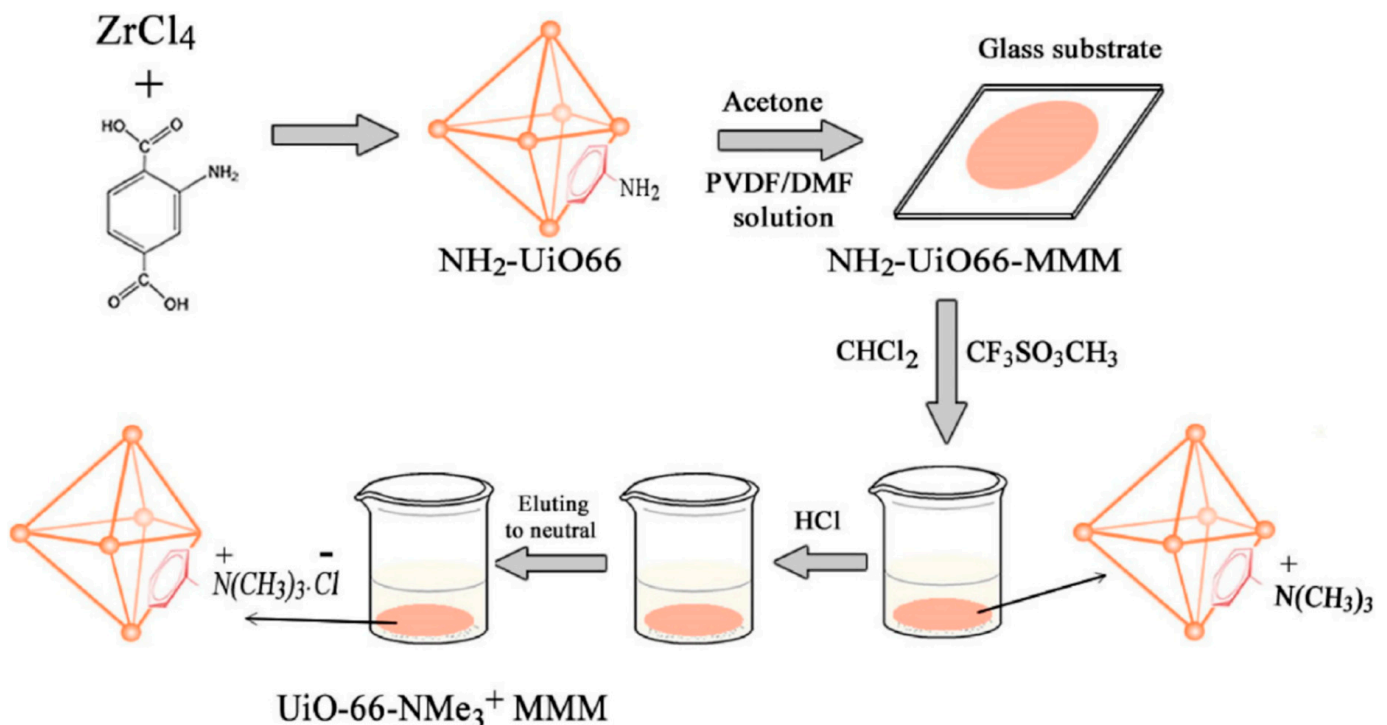


Figure 3. Illustration for the synthesis of the UiO-66-NMe₃⁺ MMM. Reprinted with permission from Ref. [88]. Copyright (2020) Elsevier.

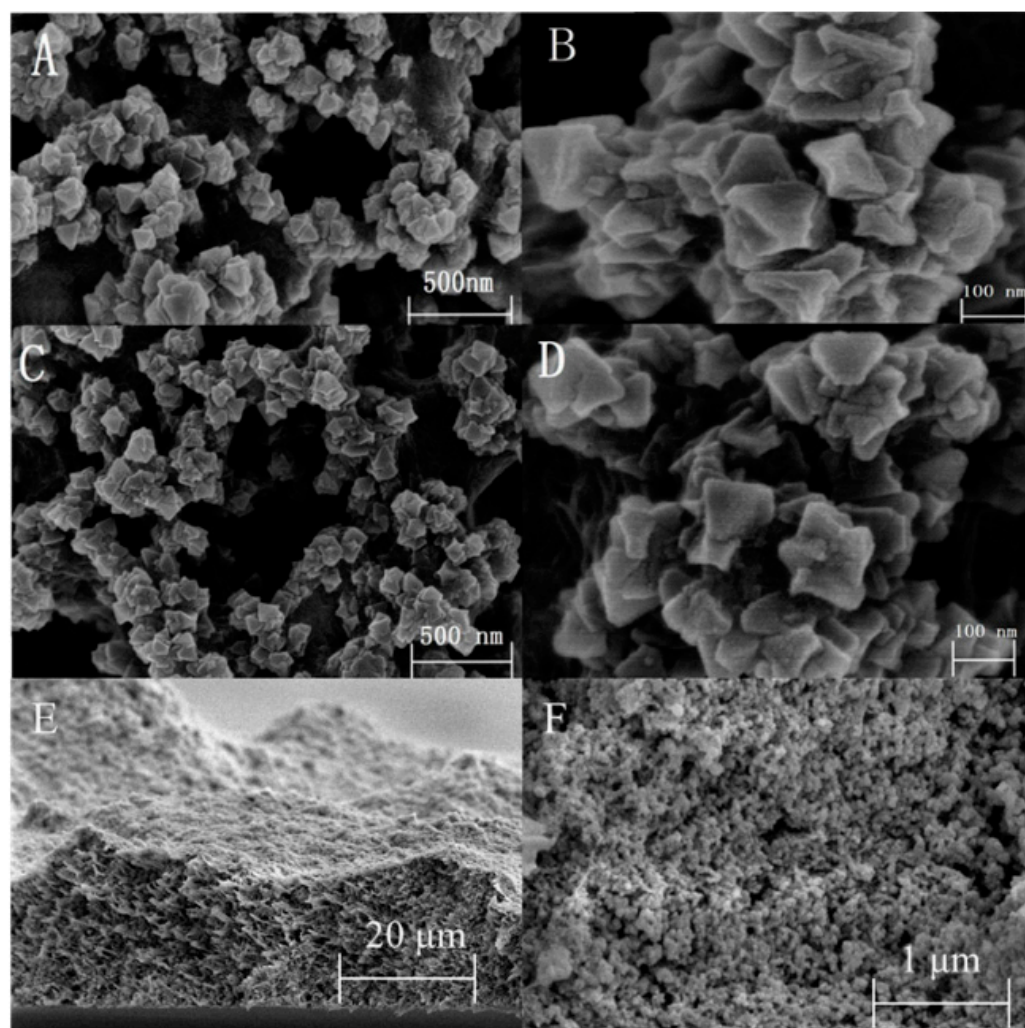


Figure 4. SEM images of UiO-66-NH₂ MMM with the scale bar of (A) 500 nm and (B) 100 nm. (C) UiO-66-NMe₃⁺ MMM with the scale bar of 500 nm and (D) 100 nm. (E) Cross-sectional SEM images of UiO-66-NMe₃⁺ MMM with the scale bar of 20 μm and (F) 1 μm. Reprinted with permission from Ref. [88]. Copyright (2020) Elsevier.

The pyridine triazole functionalized UiO-66 (UiO-66-PYTA) using UiO-66-NH₂ as a raw material was synthesized by Daliran and co-workers in 2020 [89] (Figure 5). The adsorption of Pd (II) was carried out using UiO-66-PYTA as an adsorbent. Under optimal conditions, UiO-66-PYTA had a good adsorption capacity for Pd (II), and the satisfactory limit of detection (1.9 μg/L) was obtained. The intra-day and inter-day precision are 3.6% and 1.7%. After the reuse of five cycles, the adsorption performance still had no obvious change. More interestingly, the UiO-66-PYTA that adsorbed Pd became an efficient and reusable catalyst for the Suzuki–Miyaura cross-coupling reaction. This kind of adsorption material had its application value both before and after adsorption, and successfully turns waste into treasure. It was consistent with the resource reuse advocated at present.

In 2021, a new type of nano-adsorbent, electrospun, polyacrylonitrile/nickel-based metal-organic framework (PAN/Ni-MOF) nanocomposite coating was synthesized by Amini and co-workers [90] (Figure 6). They added Ni-MOF nanoparticles to PAN nanofibers by one-step method, which improved the porosity of the adsorbents and increased the interaction between adsorbents and analytes via π - π stacking, hydrophobic contact, and hydrogen bonding. The synthesized nanofiber coating had a uniform morphology and porous structure. As a result, the adsorption performance of PAN/Ni-MOF was greatly increased. PAN/Ni-MOF was used to detect diazinon (DIZ) and chlorpyrifos (CPs). It

showed an excellent adsorption efficiency for DIZ and CPs, and the limit of detections were 0.3 ng/mL and 0.2 ng/mL. In addition, no harmful organic solvents were added in the process of synthesizing PAN/Ni-MOF, which was in line with the current theme of environmental protection.

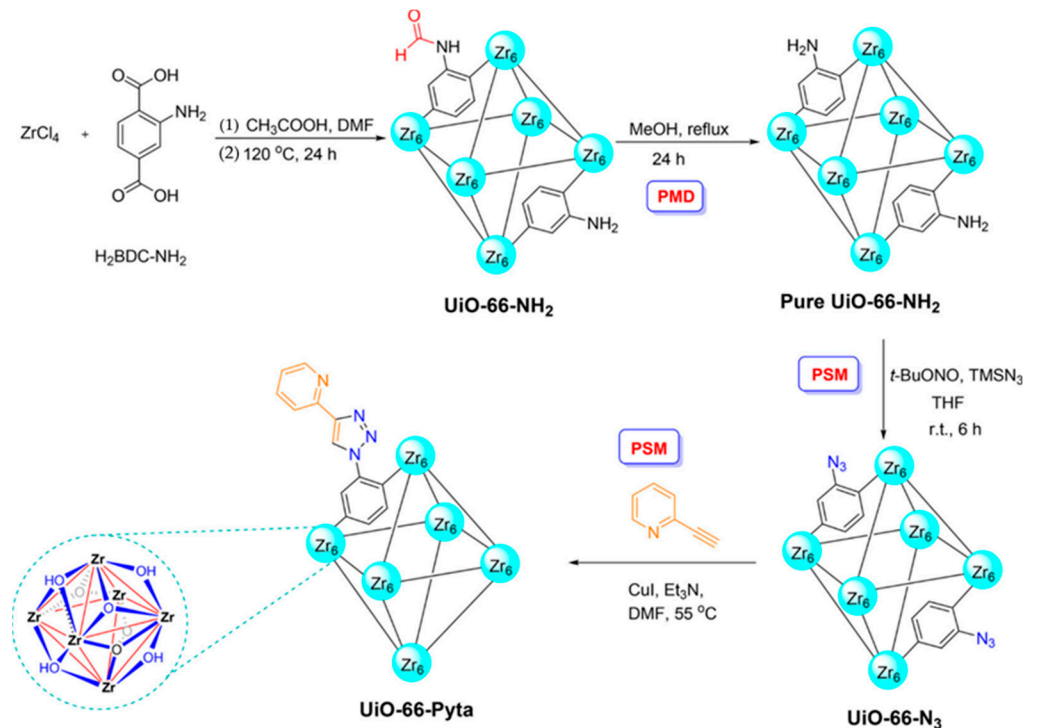


Figure 5. Schematic Synthesis: PMD and PSMs of UiO-66-NH₂ toward formation of UiO-66-Pyta. Reprinted with permission from Ref. [89]. Copyright (2020) American Chemical Society.

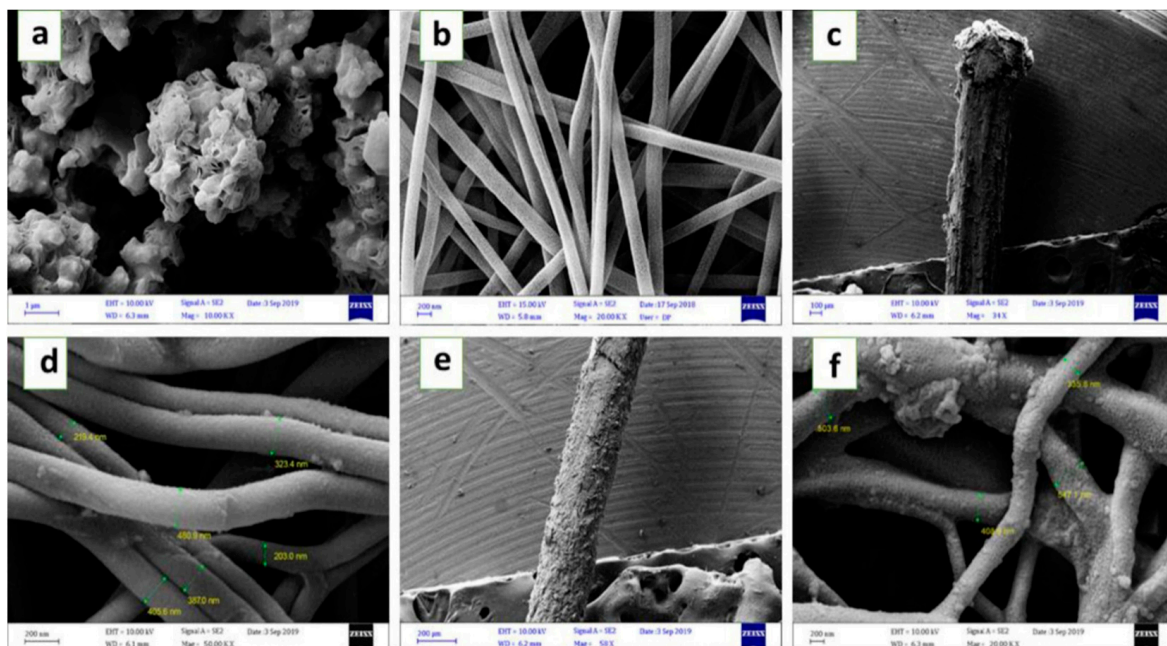


Figure 6. FESEM images of (a) Ni-MOF particles synthesized by hydrothermal method; (b) PAN nanofibers; (c,d) PAN/Ni-MOF composite nanofibers before extraction in different magnification; (e,f) electrospun PAN/Ni-MOF nanofibers after 160 times extraction in different magnification. Reprinted with permission from Ref. [90]. Copyright (2021) Elsevier.

2.2.2. Synthesis of a Covalent Organic Framework (COF) and Its Application in Sample Pretreatment

A COF is a new type of porous crystalline organic polymer formed by the polymerization of organic monomers by strong organic covalent bonds. In 2005, the crystalline porous organic polymer was synthesized by Yaghi and co-workers [91], which is the earliest COF, and then in 2007, Yaghi and co-workers [92] synthesized the first three-dimensional COF material. A COF has the advantages of large specific surface area, good stability, low density, high permanent porosity and convenient functionalization. Moreover, the structure can be adjusted, and the aperture, spatial arrangement, and functional properties of the COF can be designed according to the requirements. Functional properties can predict the design so that the COF has a very strong selectivity in the field of separation, and the large specific surface area makes the COF have a larger adsorption capacity. The synthesis of COF materials is difficult, as the construction and ordering of strong covalent bonds are problems that need to be solved. It is one of the reasons that COF materials are not widely used at present; however, with continuous study, solvothermal synthesis and ion thermal synthesis are widely used for the preparation of COF materials. Solvothermal synthesis is a commonly used method for COF synthesis. At present, most COF materials are synthesized by this method, and its specific principle is to change the molding structure of COF by adjusting the pressure, temperature, solvent ratio, and pH in the closed environment. Moreover, the ionic thermal synthesis method uses molten zinc chloride as the solvent and catalyst to make COF crystallize at high temperature.

In 2019, novel nano-titania modified COFs (NTM-COFs) modified by nano-titanium dioxide was synthesized by Zhao and co-workers [93]. The NTM-COFs were characterized by scanning electron microscopy and transmission electron microscopy, and are shown in Figure 7. NTM-COFs were used as adsorbents in the PRiME pass-through cleanup procedure for the cleanup of local anesthetic drugs in human plasma prior to liquid chromatography-tandem quadrupole mass spectrometry (LC-MS/MS) analysis. The limit of the detections obtained were less than 0.03 $\mu\text{g/L}$, and the recovery was between 88.8% and 103%. The precision and accuracy of this method were satisfactory.

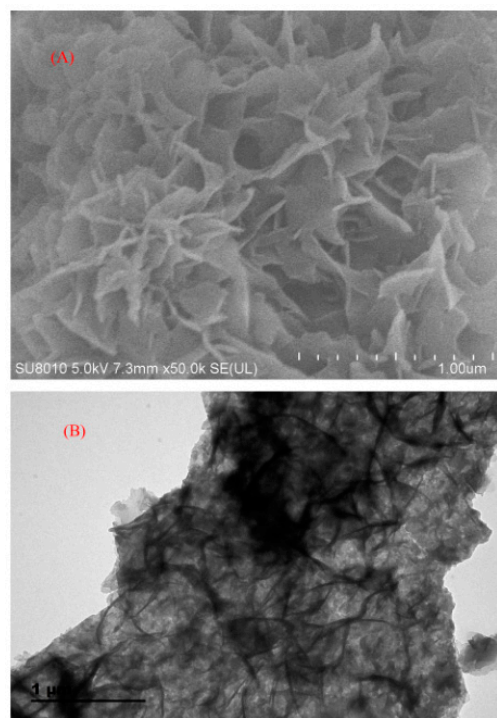


Figure 7. SEM (A) and TEM (B) images of NTM-COFs. Reprinted with permission from Ref. [93]. Copyright (2019) Elsevier.

In 2020, a novel covalent organic frameworks COF-SCU1 incorporated electrospun nanofibers (PAN@COF-SCU1 nanofibers) (Figure 8) were prepared by Wang and co-workers [94], which were used as adsorbents in pipette tip solid-phase extraction (PT-SPE) (Figure 9) for the adsorption of tetracycline antibiotics (TCs) in food prior to HPLC analysis. The prepared PAN@COF-SCU1 nanofibers showed the characteristics of electrospun nanofibers and COF-Cu1. Under the optimized conditions, PAN@COF-SCU1 nanofibers was used for extraction of tetracycline in grass carp and ducks, and then detected by PT-SPE/HPLC. The limit of detection obtained was 0.6–3 ng/mL, and inter-day and intra-day precision were less than 9.0%. The results showed that PAN@COF-SCU1 nanofibers had excellent adsorption efficiency for TCs, and the established PT-SPE/HPLC method had high precision in the determination of TCs.

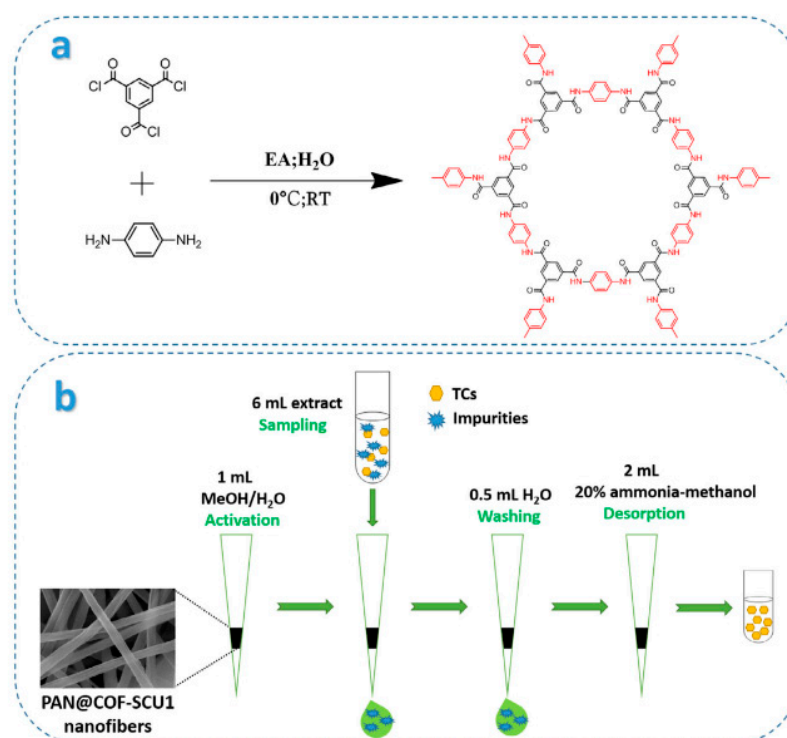


Figure 8. Schematic diagrams of (a) preparation of COF-SCU1 and (b) PT-SPE procedure for the extraction of TCs. Reprinted with permission from Ref. [94]. Copyright (2020) Elsevier.

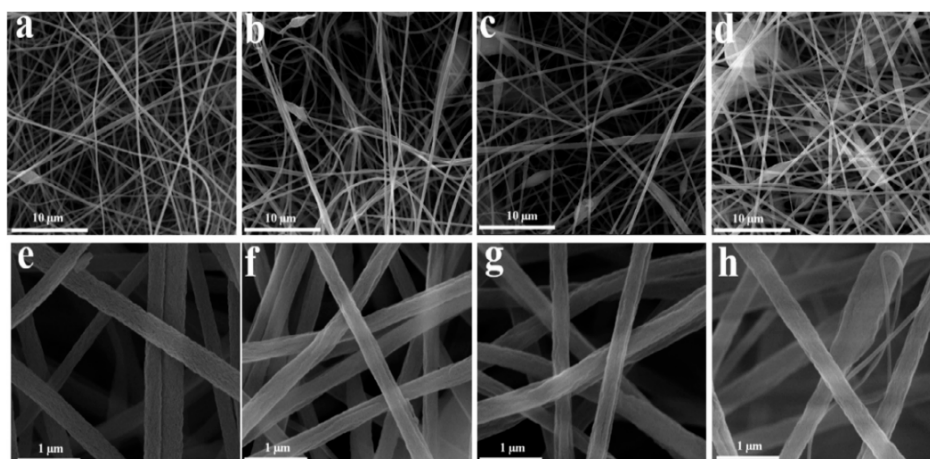


Figure 9. (a,e) SEM images of PAN nanofibers; (b,f) PAN@COF-SCU1 (0.1); (c,g) PAN@COF-SCU1 (0.2); (d,h) PAN@COF-SCU1 (0.3). Reprinted with permission from Ref. [94]. Copyright (2020) Elsevier.

In 2020, Zhu and co-workers [95] synthesized novel, petal-shaped, ionic liquid modified COF (PS-IL-COFs) particles using ionic liquid as modifier (Figure 10). They also proposed a new one step cleanup and extraction (OSCE) technique. The OSCE procedure can effectively avoid the problem of the large amount of solvent used, and the long time in liquid–liquid extraction, and can also effectively avoid the cartridge conditioning and eluting steps in SPE. Based on the advantages of this procedure, PS-IL-COFs were used as adsorbents in OSCE for the cleanup of general anesthetics in human plasma prior to the LC-MS/MS analysis. The limit of detections obtained were between 0.0048 $\mu\text{g}/\text{L}$ and 0.054 $\mu\text{g}/\text{L}$, and the recovery rate was 82.5–115%.

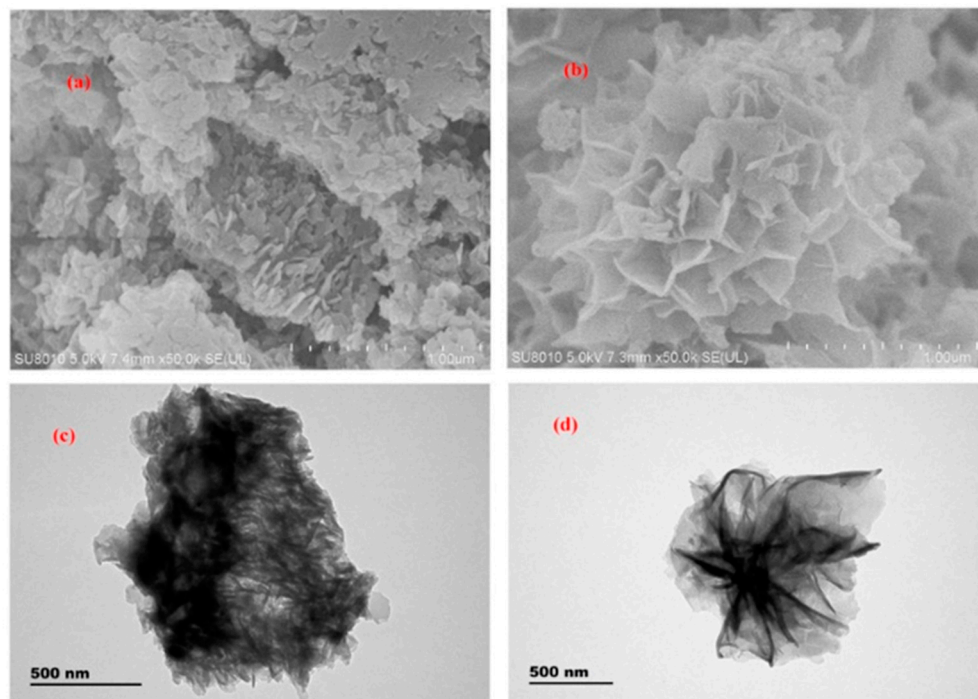


Figure 10. (a) SEM images of COFs and (b) PS-IL-COFs. (c) TEM images of COFs and (d) PS-IL-COFs. Reprinted with permission from Ref. [95]. Copyright (2020) Elsevier.

2.2.3. Synthesis of a Molecularly Imprinted Polymer (MIP) and Its Application in Sample Pretreatment

The concept of molecular imprinting was first proposed by Polykov and co-workers [96]. MIP is a new type of polymer with molecular recognition ability, which has unique pre-determination, recognition and practicability [97]. Through the template molecule, the functional monomer and the cross-linking agent can be copolymerized, then the template molecule can be removed, and so the MIP was obtained [98]. It can recognize and adsorb compounds similar to template molecules in shape, size, and chemical function [99,100]. As MIP has strong recognition function, its selectivity is very high, and MIP also has good reusability; therefore, MIP has received increasing attention [101], especially in the field of sample pretreatment. Due to its high selectivity and loading capacity, MIP can be used as an adsorbent in sample pretreatment for the extraction/pre-concentration of trace chemicals. In addition, it has the advantages of low cost, easy preparation, reusability, and high stability in various pH values and temperatures [102,103]. The preparation methods of MIP include suspension polymerization, seed polymerization, emulsion polymerization, and so on [104,105].

Suspension polymerization is the traditional polymerization method, which uses water as a continuous phase to suspend droplets in the presence of stabilizers or surfactants, and then polymerization occurs; however, the particle size of MIP prepared by suspension polymerization is uneven, and the recognition ability is poor. It may be argued that the

hydrogen bond and electrostatic interaction in water has an effect on the polymerization process. Seed polymerization is a multi-step swelling polymerization method, in which monodisperse MIP are prepared and then modified in situ; however, water is also used as the continuous phase in this method, so the reaction process may be affected by the hydrogen bond and electrostatic interaction in water. As for emulsion polymerization, it has always been considered as an effective method for the production of highly efficient and monodisperse polymerized particles, and it has been proven that it can be used for the preparation of MIP.

In 2021, a method for the extraction of rosmarinic acid (RA) using MIP was reported by Saad and co-workers [106]. First, the surface imprinted polymer was prepared by using RA as a template, and then it was used as adsorbent for SPE procedure. With the optimized MIP-SPE method (Figure 11), the recovery rate of rosemary can be stabilized at $81.96 \pm 6.33\%$. It can be seen that MIP had excellent adsorption rate on the adsorption of rosemary, and the MIP-SPE method also had further application value in sample pretreatment.

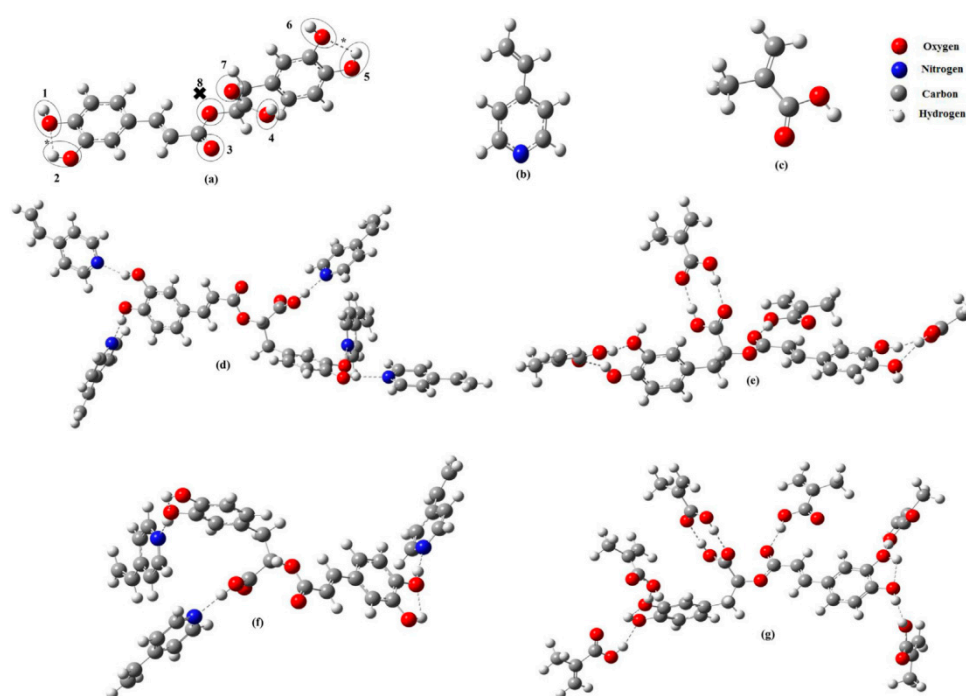


Figure 11. Computer optimized structures of (a) RA, (b) 4-VP, and (c) MAA, conformations, optimum. (d) RA-(4-VP)₅ and (e) RA-(MAA)₄ conformations assuming no intra-molecular H-bond formation, optimum (f) RA-(4-VP)₃, and (g) RA-(MAA)₆ conformations assuming intra-molecular H-bond formation. The possible active binding sites are encircled, * represents possible intra-molecular H-bonds of a distance (2.166–2.174 Å), and x represents the site incapable of H-bonding with MAA. Reprinted with permission from Ref. [106]. Copyright (2021) Elsevier.

In 2021, a novel, reversible, addition–fragmentation chain transfer polymerization method for the preparation of MIP was reported by Li and co-workers [107]. It was used as a SPE adsorbent for the extraction of four phenylarsine compounds in feed, edible chicken, and pork samples. The results showed that the recovery rate of phenylarsine compounds by the developed MIP-SPE method was between 83.4% and 95.1%.

2.2.4. Synthesis of Porous Hybrid Material and Its Application in Sample Pre-Treatment

With the continuous improvement to the requirements of analytical accuracy and the increasing complexity of analytical targets, the performance of a single material is gradually unable to meet the current needs, so researchers focus on hybrid materials, among which, the hybrid of porous materials is one of the important research directions. Graphene oxide

is one of the more popular materials in hybrid materials, because graphene oxide is rich in oxygen-containing groups, and has a π stacking interaction, thermal stability, mechanical stability, and high specific surface area.

In 2022, a novel Cu-based metal–organic framework/graphene oxide (Cu–MOF/GO) hybrid nanocomposite coated on a stainless-steel mesh using the sol–gel method was prepared by Abdar and co-workers [108]. The hybrid nanocomposite was used as semi-automatic SPE sorbent for the extraction of polycyclic aromatic hydrocarbons. The extracted PAHs were analyzed by gas chromatography-flame ionization detection (GC-FID). Under the optimal experimental conditions, the detection limit was 0.3–1.8 pg/mL, the relative recovery was between 95.1–99.5%, and the relative standard deviation (RSD%) was between 4.9–6.9%. This method combined the advantages of GO, Cu-MOF, and the sol–gel method, and thus, this hybrid nanomaterial had a variety of synergistic effects.

Moreover, an effective adsorbent of polypyrrole doped GO/COF-300 (GO/COF-300/PPy) nanocomposite was prepared for the first time by Feng and co-workers in 2022 [109]. This hybrid material was used for the adsorption of indomethacin (IDM) and diclofenac (DCF) in aqueous solution. The concentration of IDM and DCF was determined by a UV-vis spectrometer at 264 nm and 274 nm. The results showed that the adsorption efficiency of GO/COF-300/PPy composite for IDM and DCF was much higher than that of single GO and COF, and the adsorption capacity of DIM and DCF were 115 mg/g and 138 mg/g, respectively. And after 8 times of adsorption-desorption process, the adsorption efficiency of GO/COF-300/PPy composite materials for IDM and DCF decreased by 27% and 29%, indicating that GO/COF-300/PPy has good reusability and stability.

2.3. Magnetic Nanomaterials

As we know, the common ferromagnetic materials in nature are Fe_2O_3 , Fe_3O_4 , ferrites (MFe_2O_4 , $\text{M}=\text{Mn, Zn, Co, Ni, Cu}$) and so on. It has become a trend of scientific research to magnetize nano-materials and improve their properties. In recent years, many magnetic nanomaterials have been reported, such as $\gamma\text{-Fe}_2\text{O}_3$, Fe_3O_4 , Mn_3O_4 , MnO , CoFe_2O_4 , MnFe_2O_4 . The preparation methods of magnetic nanomaterials are mainly divided into three categories; (1) chemical synthesis methods include aqueous solution coprecipitation method, hydrothermal method, microemulsion method and thermal decomposition method; (2) physical synthesis methods include mechanical ball milling method and evaporation condensation method; (3) the biosynthesis method.

Magnetic nanocomposites have different properties from traditional materials, such as superparamagnetism, high coercivity, low curie temperature, and high susceptibility. With the application of magnetic field, the magnetic adsorbent can be easily separated from the matrix solution after adsorbing the target analyte; therefore, there is no need for centrifugation or filtration. Recently, MSPE has been developed rapidly. MSPE uses magnetic materials as solid-phase adsorbents, which can greatly simplify the SPE procedure and improve the extraction efficiency.

Although magnetic nanomaterials are widely used as adsorbents in MSPE, magnetic nanoparticles are prone to agglomeration due to magnetic nanometer size, large specific surface area, high surface energy and reaction activity. In order to increase the structural stability and enhance the specific binding between magnetic nanoparticles and the target analytes, the surface of magnetic particles should be functionalized. After the surface modification of magnetic particles by different methods, magnetic nanoparticles can effectively reduce the phenomenon of aggregation, enhance the stability in solution.

(1) Modification with polymer: magnetic nanoparticles have poor stability and biocompatibility, and are thus easy to be oxidized. The surface of magnetic nanoparticles can be modified by polymer materials with good biocompatibility. In most cases, the magnetic nanocomposites synthesized are core-shell structures. There are two ways to do this for magnetic nanoparticles coated with polymer. One is physical coating, that is, polymers are directly coated on the surface of magnetic nanoparticles to synthesize organic polymers in situ. Another method is chemical coating, which is to modify the surface of magnetic

nanoparticles to connect their surfaces with specific functional groups. Then the functional groups can react with polymers to form magnetic nanocomposites.

A new modification method for the preparation of N-doped magnetic covalent organic framework (N-Mag-COF) was reported by Wu and co-workers [110]. It has been evaluated in the magnetic dispersive solid phase extraction (Mag-dSPE) procedure for allergenic disperse dyes prior to LC-MS/MS analysis. Under optimal conditions, the N-Mag-COF Mag-dSPE procedure can significantly reduce the matrix effect and obtain satisfactory recoveries with RSD lower than 8.0%

A method for the synthesis of novel magnetic nanocomposites was reported by Lu and co-workers [111]. Fe_3O_4 particles functionalized by polydopamine was grafted onto Zr-MOF by layer modification, and then the hydrophobic carboxyl functionalized ionic liquids (IL-COOH) were coated onto the Fe_3O_4 @Zr-MOF magnetic particles, and the novel IL-COOH/ Fe_3O_4 @Zr-MOF magnetic nanocomposites were obtained (Figure 12). IL-COOH/ Fe_3O_4 @Zr-MOF had been used as an adsorbent for the extraction of fluoroquinolone antibiotics in environmental water samples prior to HPLC analysis. The results showed that IL-COOH/ Fe_3O_4 @Zr-MOF had an excellent adsorption efficiency for fluoroquinolones antibiotics, and the maximum adsorption capacity of ofloxacin was 438.5 mg/g, the recovery of ofloxacin in environmental water samples was between 90.0% and 110.0%, and the limit of detection was less than 0.02 $\mu\text{g/L}$.

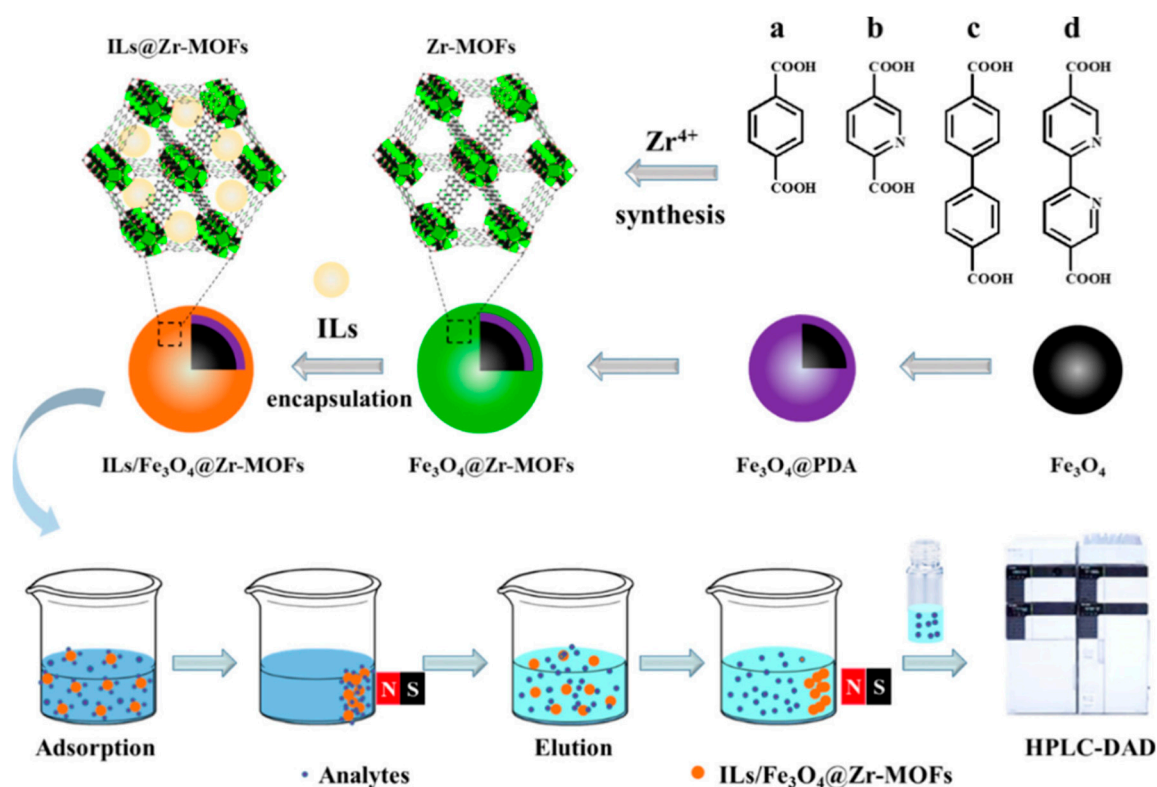


Figure 12. Preparation of ILs/ Fe_3O_4 @Zr-MOFs and MSPE Process. Reprinted with permission from Ref. [111]. Copyright (2021) American Chemical Society.

Li and co-workers [112] reported a green method for the preparation of hydrophilic magnetic MIP composites for the extraction of cyclic adenosine monophosphate (cAMP). Magnetic carbon nanotubes (MCNTs) modified by tetraethyl orthosilicate (TEOS) was embedded into the chitosan (CS) network to obtain cAMP-MIPs@MCNTs composites (Figures 13 and 14). The cAMP-MIPs@MCNTs had been used as adsorbents to extract cAMP from winter prior to HPLC analysis. The results showed that cAMP-MIPs@MCNTs have a high adsorption capacity for cAMP. The limit of detection was 5 ng/mg, and

the imprinting factor was 2.94, which indicated that cAMP-MIPs@MCNTs had excellent selectivity for the template molecules.

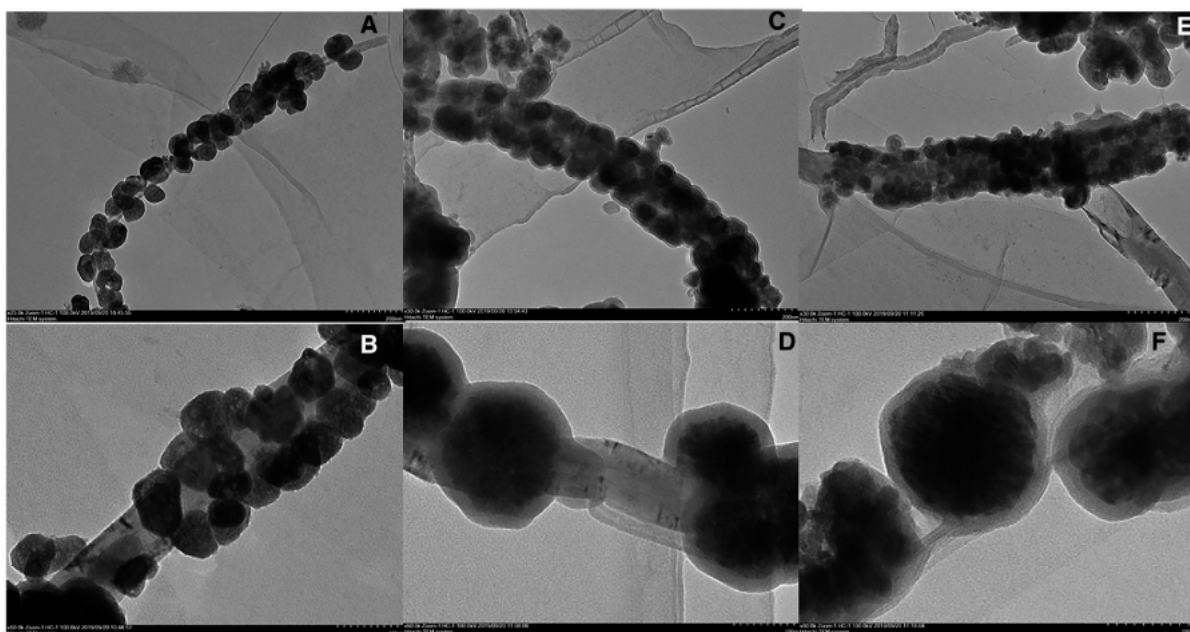


Figure 13. (A,B) TEM images of the prepared MCNTs, (C,D) TEOS@MCNTs, and (E,F) cAMP-MIPs@MCNTs. Reprinted with permission from Ref. [112]. Copyright (2021) Weinheim.

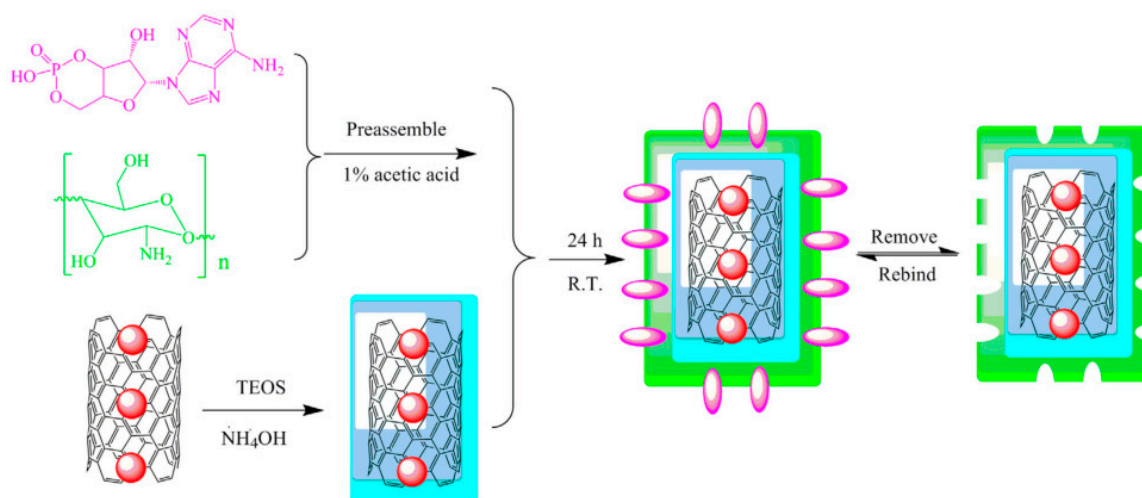


Figure 14. The synthesis procedure of cAMP-MIPs@MCNTs. Reprinted with permission from Ref. [112]. Copyright (2021) Weinheim.

(2) Modification with carbon materials: carbon materials have high thermal and chemical stability and good biocompatibility. Magnetic nanoparticles coated with carbon materials can not only prevent the agglomeration of nanoparticles, but also prevent oxidation corrosion and enhance their stability.

In 2018, a novel double-layered pipette tip magnetic dispersive solid phase extraction (DPT-MSPE), based on polyamide functionalized magnetic carbon nanotubes (PAMAM@Mag-CNTs) (Figure 15), was synthesized by Cheng and co-workers [113]. It was applied to the adsorption of fifteen toxic alkaloids in vegetables and meat. Under the optimal conditions, the satisfactory recoveries were between 83.4% and 125%, and the RSD was less than 8%.

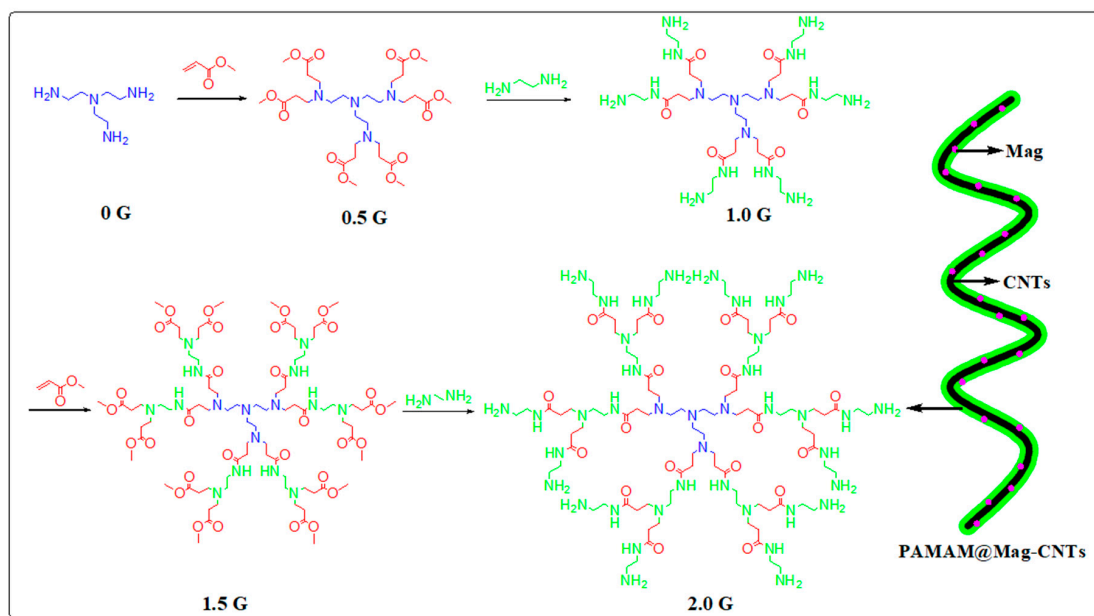


Figure 15. The synthetic process of PAMAM. Reprinted with permission from Ref. [113]. Copyright (2018) Royal Society Chemistry.

In 2018, an enhanced cleanup efficiency hydroxy functionalized-magnetic GO (EH-MAG-GO) modified by hydroxyl group was successfully synthesized by Ma and co-workers (Figures 16 and 17) [9]. EH-MAG-GO was used as an adsorbent in the PRiME pass-through cleanup procedure for the cleanup of strychnine and brucine prior to LC-MS/MS analysis. Under the optimized conditions, the limit of detections for strychnine and brucine were 0.088 $\mu\text{g/L}$ and 0.092 $\mu\text{g/L}$, and the recovery was 89.4–118%. Notably, the EH-Mag-GO can be reused (20 times) without much sacrifice of cleanup efficiency, and the validation results demonstrated the applicability of the EH-MAG-GO PRiME pass-through cleanup procedure for clinical studies.

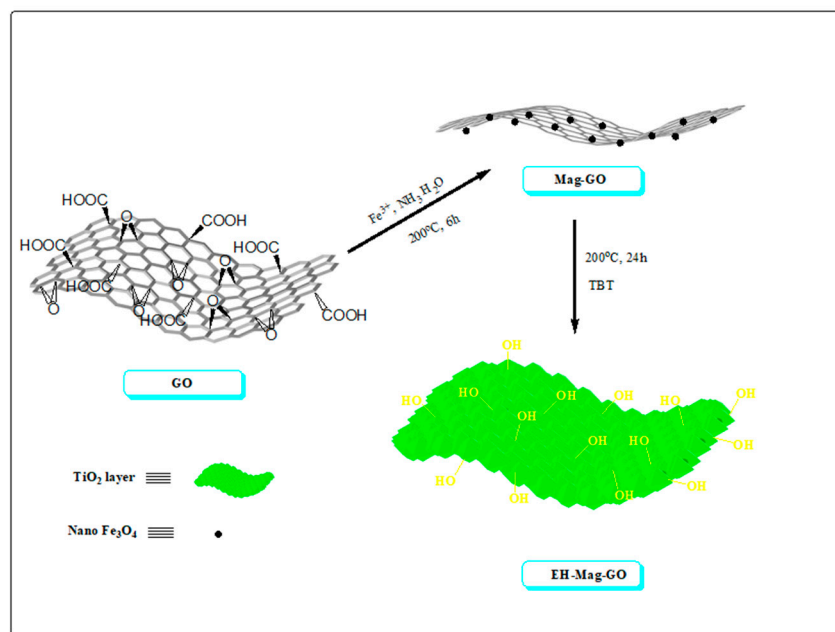


Figure 16. The preparation procedure of EH-Mag-GO. Reprinted with permission from Ref. [9]. Copyright (2018) Elsevier.

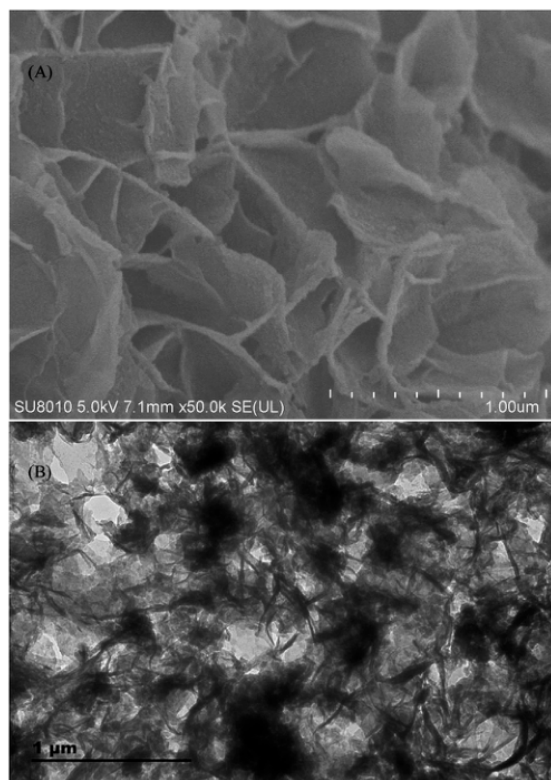


Figure 17. SEM (A) and TEM (B) images of EH-Mag-GO. Reprinted with permission from Ref. [9]. Copyright (2018) Elsevier.

GO-Fe₃O₄ magnetic nanocomposites, using a simple chemical coprecipitation method, was successfully synthesized by Lu and co-workers [114]. In this method, Fe₃O₄ formed by the co-precipitation of Fe²⁺ and Fe³⁺ was successfully bonded to the GO with the aid of the -COOH under ultrasound. The preparation process of GO-Fe₃O₄ was shown in Figure 18. GO-Fe₃O₄ was applied to SPME as an adsorbent to extract eight psychoactive drugs from urine prior to LC-MS/MS analysis. The limit of detection of the analytical method was 0.02–0.2 μg/L, and the intra-day and inter-day RSD were in the range of 2.7–13.1% and 3.9–13.7%, respectively.

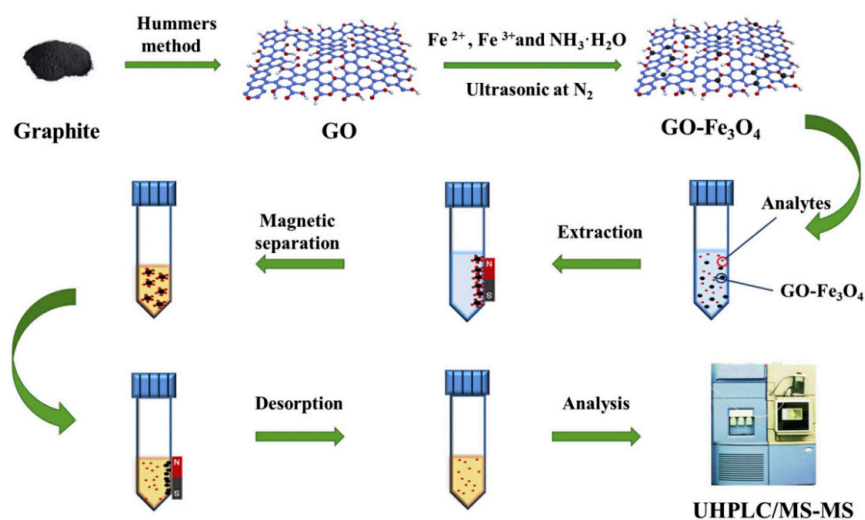


Figure 18. Schematic illustration of the synthesis of GO-Fe₃O₄ and MSPE procedure for analysis of the eight psychoactive drugs. Reprinted with permission from Ref. [114]. Copyright (2020) Elsevier.

Furthermore, the performance of nanomaterials as adsorbents in combination with other technologies have been summarized, and the results are shown in Table 1. As shown in the table, the proposed sample pretreatment with nanomaterials as adsorbents give much lower LODs of various chemical analytes.

Table 1. The summary of the properties of nanomaterials as adsorbents in combination with other technologies.

Sample	Target Analyte	Adsorbent	Pretreatment Method	Detection	LOD ($\mu\text{g/mL}$)	Recovery (%)	Ref.
Crude oil	As(III) As(V)	C60-SESMP-Fe ₃ O ₄	MSPE	ICP-OES	0.047–0.032	96.5–98.0	[48]
Wild rice	Pb (II)	ox-MWCNTs/ batophenanth	DMSPE	FAAS	0.25	93.8	[60]
Sewage water	U(VI)	Br-PADAP/MWCNT	MSPE	ICP-AES	0.14	99.7	[61]
Cosmetics	Parabens	MoS ₂ /GO	DSPE	UPLC-PDA	0.40~2.3	91.3–124	[71]
Sewage water	PCAs	UIO-66-NMe ₃ ⁺ MMM	DME	UHPLC-MS/MS	0.030–0.59	80.1–117	[88]
Tap water	Pd(II)	UIO-66-Pyta	SPE	ICP-AES	1.9	99.0	[89]
Duck, Grass Carp	TCs	PAN@COF-SCU1	PT-SPE	HPLC	0.60–3.0	84.0–117	[94]
Human Plasma prior	Anesthetics	PS-IL-COFs	OSCE	LC-MS/MS	0.016–0.18	82.5–115	[95]
Rice, apples, green groceries	PCAs	TAPT-DHTA-COF	SPE	LC-MS/MS	0.0070–0.030	81.2–107	[96]
River water	OPPS	PAN/Ni-MOF	HS-SPME	CD-IMS	0.20–0.30	87.0–98.0	[90]
River water	FQS	IL-COOH/Fe ₃ O ₄ @Zr-MOF	MSPE	HPLC-DAD	<0.020	90.0–110	[111]
Meat, vegetables	Toxic alkaloids	PAMAM@Mag-CNTs	DPT-MSPE	UFLC-MS/MS	0.011~0.329	83.4–125	[113]
Urine	Psychoactive drugs	GO-Fe ₃ O ₄	MSPE	UHPLC-MS/MS	0.020–0.20	80.4–105	[114]

2.4. Regeneration and Reproducibility of Nanomaterials

When nanomaterials are used as adsorbents, the regeneration and reproducibility of the adsorbents are very important evaluation indicators.

In order to achieve good regeneration, the selection of eluent is very important, which is also the key to the optimization of the solid phase extraction process. As for the reproducibility of the nanomaterial, it is necessary to carry out parallel experiments, and then calculate the relative deviation of these parallel experiments. For example, Zhao and co-workers [115] reported a novel, three-dimensional, interconnected, magnetic, chemically modified graphene oxide (3D-Mag-CMGO) for the enrichment of dispersed dyes in water samples. The 3D-Mag-CMGO-adsorbed could be conveniently regenerated by using 5.0% ammonia solution/methanol (*v/v*) and water as an eluent, allowing for them to be used repeatedly for Mag-dSPE method. After adsorption–desorption experiments, the results showed that 3D-Mag-CMGO could be reused at least ten times without much sacrifice of the extraction efficiency. In addition, six parallel experiments were carried out, and the relative deviation of the recovery rate of the target substance were between 4.6–8.0%. In 2018 [116], they tested the regeneration and reproducibility of quaternary ammonium modified magnetic carboxyl-carbon nanotubes (QA-Mag-CCNTs) and found that ammonia solution/water (5.0% *v/v*) was the best eluent. After desorption, the recovery rate of the target substance could reach 89.2%. Moreover, after 20 times of adsorption–desorption experiments, the adsorption efficiency of the nanomaterial to the target did not decrease significantly. Furthermore, after eight parallel experiments, the relative standard deviation was between 3.6–7.0%, and in the same year, Zhang and co-workers tested the regeneration and reproducibility of the three-dimensional ionic liquid-ferrite functionalized graphene oxide nanocomposite (3D-IL-Fe₃O₄-GO) [117]. For optimal regeneration, they conducted a lot of experiments. Results showed that the adsorbed 3D-IL-Fe₃O₄-GO could be conveniently regenerated by washing with toluene and water sequentially. In addition, 3D-IL-Fe₃O₄-GO could be reused at least 10 times with nearly invariable quantitative efficiency. For reproducible detection, five batches of 3D-IL-Fe₃O₄-GO were prepared and applied in five parallel sets of experiments, the relative deviation is between 4.5% and 8.6%.

3. Conclusions and Outlook

In this review, we briefly summarize the latest progress in the preparation of nanomaterials and their applications in sample pretreatment methods. Numerous selected nanomaterials have been described in detail. Combined with these studies, it can be proved that the application of nanomaterials in sample pretreatment has great potential in the future. Although the adsorption efficiency, selectivity, and reproducibility of nanomaterials are better than those of traditional adsorbents, there are still some problems and challenges in nanomaterials that need to be overcome.

(1) The structure of carbon nanomaterials and magnetic nanomaterials are relatively simple, and the selectivity is poor, which greatly affects its practical application. In order to improve the selectivity of carbon nanomaterials and magnetic nanomaterials, multi-modification of specific functional groups should be considered.

(2) The synthesis method of MOFs' and COFs' nanomaterials are complex, and some expensive or toxic reagents may be used in the synthesis process. Reducing the synthesis complexity of existing nanomaterials and increasing its reproducibility and repeatability are key factors in the future study.

(3) For the MIP nanomaterials, it takes long incubation times to induce the binding of the analyte onto the recognition sites on the MIP surface, and these recognition sites will also bind to some molecules with similar structure to the target analyte, thus affecting the selectivity of MIP nanomaterials. In addition, the non-compound forms of MIP are very limited studies at present, which limits its scope of application. The research on the non-complex form of MIP should be strengthened to further understand the adsorption mechanism of MIP, so as to find ways to improve its selective ability to identify target analytes.

Author Contributions: Writing-original draft preparation, W.-X.L.; writing-review and editing, Y.-G.Z.; supervision, S.S.; project administration, M.-L.Y. and Y.Z.; funding acquisition, Y.L. All authors have read and agreed to the published version of the manuscript.

Funding: This research was funded by Zhejiang Provincial Natural Science Foundation (No. LY20B070007), and the APC was funded by Zhejiang Provincial Key Research and Development Project (No. 2021C03176).

Data Availability Statement: Not applicable.

Acknowledgments: We would like to thank the Zhejiang Provincial Natural Science Foundation (No. LY20B070007), Zhejiang Provincial Key Research and Development Project (No. 2021C03176), the top young talents of the ten thousand talents program of the Zhejiang Province (ZJWR0308003), the State Key Laboratory of Environmental Chemistry and Ecotoxicology, Research Center for Eco-Environmental Sciences, and the Chinese Academy of Sciences (No. KF2021-24), the Zhejiang University Foundation(2021XZ011). The funders had no role in the study design, data collection, analysis, decision to publish, or preparation of the manuscript.

Conflicts of Interest: The authors declare no conflict of interest.

Abbreviations

CD-IMS	corona discharge ion mobility spectrometry
ICP-AES	inductively coupled plasma atomic emission spectrometer
PT-SPE	pipette tip solid-phase extraction
ox-MWCNTs	oxidized multiwalled carbon nanotubes
DMSPE	dispersive micro-solid phase extraction
DLLME	dispersive liquid-liquid microextraction
SPE	solid-phase extraction
HPLC	high-performance liquid chromatography
ICP-OES	Inductively Coupled Plasma Optical-Emission Spectrometry
ESMP	Eggshell membrane protein
SESMP	soluble eggshell membrane protein

OPPs	organophosphorus pesticides
DIZ	diazinon
CPs	chlorpyrifos
CD-IMS	corona discharge ion mobility spectrometry
HS-SPME	headspace solid-phase microextraction
IL-COOH	the hydrophobic carboxyl-functionalized ionic liquid
FQs	fluoroquinolone antibiotics
Br-PADAP	[2-(5-Bromo-2-pyridylazo)-5-(diethylamino)phenol]
PSM	postsynthetic modification
SWCNTs	single-walled carbon nanotubes
MWCNTs	multi-walled carbon nanotubes
CVD	chemical vapor deposition
FAAS	flame atomic absorption spectrometry
GO	graphene oxide
CS	chitosan
MoS ₂ /GO	molybdenum disulfide-graphene oxide composite
MOFs	metal-organic frameworks
MMM	mixed-matrix membrane
PCAs	phenoxy carboxylic acids
DME	dispersive membrane extraction
COF	covalent organic framework
NTM-COFs	nano-titania modified covalent organic frameworks
MSPE	magnetic solid-phase extraction
HPLC	high performance liquid chromatography
TCs	Tetracycline antibiotics
PT-SPE	Pipette tip solid-phase extraction
PAN@COF-SCU1	polyacrylonitrile@COFs
PAN	polyacrylonitrile
LC-MS/MS	liquid chromatography-tandem quadrupole mass spectrometry
dSPE	dispersive solid phase extraction
OSCE	one step cleanup and extraction
LODs	limit of detections
MIP	molecularly imprinted polymer
RA	rosmarinic acid
cAMP	cyclic adenosine monophosphate
TEOS	tetraethyl orthosilicate
PAMAM@Mag-CNTs	polyamidoamine-functionalized magnetic carbon nanotubes
GO-Fe ₃ O ₄	graphene oxide-Fe ₃ O ₄
RSD	relative standard deviations
PS-IL-COFs	petal-shaped ionic liquids modified covalent organic frameworks
DPT-MSPE	double layer pipette tip magnetic dispersive solid phase extraction
UFLC-MS/MS	ultra-fast liquid chromatography-tandem quadrupole mass spectrometry
PAN/Ni-MOF	electrospun polyacrylonitrile/nickel-based metal-organic framework nanocomposite
EH-Mag-GO	enhanced cleanup efficiency hydroxy functionalized-magnetic graphene oxide
UPLC-PDA	Ultra-high-performance liquid chromatography with photodiode array detector
Cu-MOF/GO	Cu-based metal-organic framework/graphene oxide
GC-FID	gas chromatography-flame ionization detection
GO/COF-300/PPy	polypyrrole doped GO/COF-300
IDM	indomethacin
DCF	diclofenac
QA-Mag-CCNTs	quaternary ammonium modified magnetic carboxyl-carbon nanotubes
3D-IL-Fe ₃ O ₄ -GO	three-dimensional ionic liquid-ferrite functionalized graphene oxide nanocomposite

References

1. Azzouz, A.; Kailasa, S.K.; Lee, S.S.; Rascon, A.J.; Ballesteros, E.; Zhang, M.; Kim, K.H. Review of nanomaterials as sorbents in solid-phase extraction for environmental samples. *TrAC Trends Anal. Chem.* **2018**, *108*, 347–369. [[CrossRef](#)]
2. Ridgway, K.; Lalljie, S.P.D.; Smith, R.M. Sample preparation techniques for the determination of trace residues and contaminants in foods. *J. Chromatogr. A* **2007**, *1153*, 36–53. [[CrossRef](#)] [[PubMed](#)]
3. Nasiri, M.; Ahmadzadeh, H.; Amiri, A. Sample preparation and extraction methods for pesticides in aquatic environments: A review. *TrAC Trends Anal. Chem.* **2020**, *123*, 72–97. [[CrossRef](#)]
4. Płotka-Wasyłka, J.; Szczepańska, N.; de la Guardia, M.; Namieśnik, J. Modern trends in solid phase extraction: New sorbent media. *TrAC Trends Anal. Chem.* **2016**, *77*, 23–43. [[CrossRef](#)]
5. Kusano, M.; Sakamoto, Y.; Natori, Y.; Miyagawa, H.; Tsuchihashi, H.; Ishii, A.; Zaitzu, K. Development of “Quick-DB forensic”: A total workflow from QuEChERS-dSPE method to GC-MS/MS quantification of forensically relevant drugs and pesticides in whole blood. *Forensic Sci. Int.* **2019**, *300*, 125–135. [[CrossRef](#)]
6. Vijayasathy, S.; Baduel, C.; Hof, C.; Bell, I.; Del Mar Gomez Ramos, M.; Ramos, M.J.G.; Kock, M.; Gaus, C. Multi-residue screening of non-polar hazardous chemicals in green turtle blood from different foraging regions of the Great Barrier Reef. *Sci. Total Environ.* **2019**, *652*, 862–868. [[CrossRef](#)]
7. Shin, Y.; Lee, J.; Lee, J.H.; Lee, J.; Kim, E.; Liu, K.H.; Lee, H.S.; Kim, J.H. Validation of a multiresidue analysis method for 379 pesticides in human serum using liquid chromatography-tandem mass spectrometry. *J. Agric. Food Chem.* **2018**, *66*, 3550–3560. [[CrossRef](#)]
8. Taliansky-Chamudis, A.; Gomez-Ramirez, P.; Leon-Ortega, M.; Garcia-Fernandez, A.J. Validation of a QuEChERS method for analysis of neonicotinoids in small volumes of blood and assessment of exposure in Eurasian eagle owl (*Bubo bubo*) nestlings. *Sci. Total Environ.* **2017**, *595*, 93–100. [[CrossRef](#)]
9. Ma, J.B.; Qiu, H.W.; Rui, Q.H.; Liao, Y.F.; Chen, Y.M.; Xu, J.; Zhang, Y.; Zhu, Y.; Zhao, Y.G. Enhanced cleanup efficiency hydroxy functionalized-magnetic graphene oxide and its comparison with magnetic carboxyl-graphene for PRiME pass-through cleanup of strychnine and brucine in human plasma samples. *Anal. Chim. Acta* **2018**, *1020*, 41–50. [[CrossRef](#)]
10. Zhang, S.; Zhao, Y.; Li, H.; Zhou, S.; Chen, D.; Zhang, Y.; Yao, Q.; Sun, C. A simple and high-throughput analysis of amatoxins and phallotoxins in human plasma, serum and urine using UPLC-MS/MS combined with PRiME HLB μ Elution platform. *Toxins* **2016**, *8*, 128. [[CrossRef](#)]
11. Miao, H.; Huang, Y.; Ma, C.; Li, J.; Zhao, Y.; Wu, Y. Ultra-high-performance liquid chromatography-isotope dilution tandem mass spectrometry for the determination of phthalate secondary metabolites in human serum based on solid-phase extraction. *J. AOAC Int.* **2019**, *102*, 271–277. [[CrossRef](#)] [[PubMed](#)]
12. Wojnicz, A.; Belmonte, C.; Koller, D.; Ruiz-Nuno, A.; Roman, M.; Ochoa, D.; Ruiz-Nuno, A.; Roman, M.; Ochoa, D.; Santos, F.A. Effective phospholipids removing microelution-solid phase extraction LC-MS/MS method for simultaneous plasma quantification of aripiprazole and dehydro-aripiprazole: Application to human pharmacokinetic studies. *J. Pharmaceut. Biomed.* **2018**, *151*, 116–125. [[CrossRef](#)] [[PubMed](#)]
13. Soriano, M.L.; Zougagh, M.; Valcarcel, M.; Rios, A. Analytical nanoscience and nanotechnology: Where we are and where we are heading. *Talanta* **2018**, *177*, 104–121. [[CrossRef](#)] [[PubMed](#)]
14. Yilmaz, E.; Soylak, M. 15-Functionalized nanomaterials for sample preparation methods. In *Handbook of Nanomaterials in Analytical Chemistry*; Elsevier: Amsterdam, The Netherlands, 2020; pp. 375–413.
15. Zhang, B.T.; Zheng, X.X.; Li, H.F.; Lin, J.M. Application of carbon-based nanomaterials in sample preparation: A review. *Anal. Chim. Acta* **2013**, *784*, 1–17. [[CrossRef](#)] [[PubMed](#)]
16. Karimi-Maleh, H.; Kumar, B.G.; Rajendran, S.; Qin, J.; Vadivel, S.; Durgalakshmi, D.; Gracia, F.; Soto-Moscoso, M.; Orooji, Y.; Karimi, F. Tuning of metal oxides photocatalytic performance using Ag nanoparticles integration. *J. Mol. Liq.* **2020**, *314*, 113588. [[CrossRef](#)]
17. Karimi-Maleh, H.; Shafieizadeh, T.; Taher, M.A.; Opoku, F.; Kiarri, E.M.; Opoku, F.; Kiarri, E.M.; Govender, P.P.; Ranjbari, S.; Rezapour, M.; et al. The role of magnetite/graphene oxide nano-composite as a high-efficiency adsorbent for removal of phenazopyridine residues from water samples, an experimental/theoretical investigation. *J. Mol. Liq.* **2020**, *298*, 112040. [[CrossRef](#)]
18. Ahmadi, M.; Elmongy, H.; Madrakian, T.; Abdel-Rehim, M. Nanomaterials as sorbents for sample preparation in bioanalysis: A review. *Anal. Chim. Acta* **2017**, *958*, 1–21. [[CrossRef](#)]
19. Wang, J.L.; Liu, G.H.; Zhang, X.R. Recent developments of nanomaterials as sorbents. *Chin. J. Anal. Chem.* **2005**, *33*, 1787–1793.
20. Zhong, C.J.; Yang, B.; Jiang, X.; Li, J. Current progress of nanomaterials in molecularly imprinted electrochemical sensing. *Crit. Rev. Anal. Chem.* **2018**, *48*, 15–32. [[CrossRef](#)]
21. Zhu, Y.; Liu, X.; Hu, Y.; Wang, R.; Chen, M.; Wu, J.; Wang, Y.; Kang, S.; Sun, Y.; Zhu, M. Behavior, remediation effect and toxicity of nanomaterials in water environments. *Environ. Res.* **2019**, *174*, 54–60. [[CrossRef](#)]
22. Saleh, T.A. Trends in the sample preparation and analysis of nanomaterials as environmental contaminants. *Anal. Chem.* **2020**, *28*, 1–10. [[CrossRef](#)]
23. Khan, W.A.; Arain, M.B.; Soylak, M. Nanomaterials-based solid phase extraction and solid phase microextraction for heavy metals food toxicity. *Food Chem. Toxicol.* **2020**, *145*, 111704. [[CrossRef](#)] [[PubMed](#)]

24. Ruiz-Palomero, C.; Soriano, M.L.; Valcarcel, M. Nanocellulose as analyte and analytical tool: Opportunities and challenges. *TrAC Trends Anal. Chem.* **2017**, *87*, 1–18. [[CrossRef](#)]
25. Westerho, P.; Alvarez, P.; Li, Q.; Torresdey, J.G.; Zimmerman, J. Overcoming implementation barriers for nanotechnology in drinking water treatment. *Environ. Sci.-Nano* **2016**, *3*, 1241–1253. [[CrossRef](#)]
26. Yang, J.; Li, J.Y.; Qiao, J.Q.; Lian, H.Z.; Chen, H.Y. Solid phase extraction of magnetic carbon doped Fe₃O₄ nanoparticles. *J. Chromatogr. A* **2014**, *1325*, 8–15. [[CrossRef](#)]
27. Zhang, S.; Niu, H.; Zhang, Y.; Liu, J.; Shi, Y.; Zhang, X.; Cai, Y. Biocompatible phosphatidylcholine bilayer coated on magnetic nanoparticles and their application in the extraction of several polycyclic aromatic hydrocarbons from environmental water and milk samples. *J. Chromatogr. A* **2012**, *1238*, 38–45. [[CrossRef](#)]
28. Zhao, X.; Liu, S.L.; Wang, P.F.; Tang, Z.; Niu, H.; Cai, Y.; Wu, F.C.; Wang, H.; Meng, W.; Giesy, J.P. Surfactant-modified flowerlike layered double hydroxide-coated magnetic nanoparticles for preconcentration of phthalate esters from environmental water samples. *J. Chromatogr. A* **2015**, *1414*, 22–30. [[CrossRef](#)]
29. Wang, W.D.; Huang, Y.M.; Shu, W.Q.; Cao, J. Multiwalled carbon nanotubes as adsorbents of solid-phase extraction for determination of polycyclic aromatic hydrocarbons in environmental waters coupled with high-performance liquid chromatography. *J. Chromatogr. A* **2007**, *1173*, 27–36. [[CrossRef](#)]
30. Hu, X.; Li, J.; Chen, Q.Q.; Lin, Z.F.; Yin, D.Q. Combined effects of aqueous suspensions of fullerene and humic acid on the availability of polycyclic aromatic hydrocarbons: Evaluated with negligible depletion solid-phase microextraction. *Sci. Total Environ.* **2014**, *493*, 12–21. [[CrossRef](#)]
31. Cai, M.Q.; Su, J.; Hu, J.Q.; Wang, Q.; Dong, C.Y.; Pan, S.D.; Jin, M.C. Planar graphene oxide-based magnetic ionic liquid nanomaterial for extraction of chlorophenols from environmental water samples coupled with liquid chromatography–tandem mass spectrometry. *J. Chromatogr. A* **2016**, *1459*, 38–46. [[CrossRef](#)]
32. Han, Q.; Liang, Q.L.; Zhang, X.Q.; Yang, L.; Ding, M.Y. Graphene aerogel based monolith for effective solid-phase extraction of trace environmental pollutants from water samples. *J. Chromatogr. A* **2016**, *1447*, 39–46. [[CrossRef](#)] [[PubMed](#)]
33. Abujaber, F.; Zougagh, M.; Jodeh, S.; Ríosb, Á.; Javier, F.; Bernardo, G.; Martín-Doimeadios, R.C.R. Magnetic cellulose nanoparticles coated with ionic liquid as a new material for the simple and fast monitoring of emerging pollutants in waters by magnetic solid phase extraction. *Microchem. J.* **2018**, *137*, 490–495. [[CrossRef](#)]
34. Lian, L.; Lv, J.L.; Wang, X.Y.; Lou, D.W. Magnetic solid–phase extraction of tetracyclines using ferrous oxide coated magnetic silica microspheres from water samples. *J. Chromatogr. A* **2018**, *1534*, 1–9. [[CrossRef](#)] [[PubMed](#)]
35. Shahrman, M.S.; Ramachandran, M.R.; Zain, N.N.M.; Mohamad, S.; Manan, N.S.A.; Mohamad, S.; Manan, N.S.A.; Yaman, S.M. Polyaniline-dicationic ionic liquid coated with magnetic nanoparticles composite for magnetic solid phase extraction of polycyclic aromatic hydrocarbons in environmental samples. *Talanta* **2018**, *178*, 211–222. [[CrossRef](#)] [[PubMed](#)]
36. Lucena, R.; Simonet, B.M.; C’ardenas, S.; Valc’ arcel, M. Potential of nanoparticles in sample preparation. *J. Chromatogr. A* **2011**, *1218*, 620–637. [[CrossRef](#)] [[PubMed](#)]
37. Zhang, Y.; Yang, H.N.; Yu, Y.B.; Zhang, Y. Application of nanomaterials in proteomics-driven precision medicine. *Theranostics* **2022**, *12*, 2674–2686. [[CrossRef](#)]
38. Ma, C.X.; Xie, L.; Wang, X.; Liang, K.; Kong, B. Interfacial assembly of functional mesoporous nanomaterials for laser desorption/ionization mass spectrometry. *Nano Today* **2022**, *42*, 101365. [[CrossRef](#)]
39. Kroto, H.W.; Heath, J.R.; O’Brien, S.C.; Curl, R.F.; Smalley, R.E. C₆₀: Buckminsterfullerene. *Nature* **1985**, *318*, 162–163. [[CrossRef](#)]
40. Iijima, S. Helical microtubules of graphitic carbon. *Nature* **1991**, *354*, 56–58. [[CrossRef](#)]
41. Novoselov, K.S.; Geim, A.K.; Morozov, S.V.; Jiang, D.; Zhang, Y.; Dubonos, S.V.; Grigorieva, I.V.; Firsov, A.A. Electric field effect in atomically thin carbon films. *Science* **2004**, *306*, 666–669. [[CrossRef](#)]
42. Wen, Y.; Chen, L.; Li, J.; Liu, D.; Chen, L. Recent advances in solid-phase sorbents for sample preparation prior to chromatographic analysis. *TrAC Trends Anal. Chem.* **2014**, *59*, 26–41. [[CrossRef](#)]
43. Hayashi, T.; Kim, Y.A.; Natsuki, T.; Endo, M. Mechanical properties of carbon nanomaterials. *Chem. Phys. Chem.* **2007**, *8*, 999–1004. [[CrossRef](#)] [[PubMed](#)]
44. Khorshidi, M.; Asadpour, S.; Sarmast, N.; Dinari, M. A review of the synthesis methods, properties, and applications of layered double hydroxides/carbon nanocomposites. *J. Mol. Liq.* **2022**, *348*, 118399. [[CrossRef](#)]
45. Krätschmer, W.; Lamb, L.D.; Fostiropoulos, K.; Huffman, D.R. C₆₀: A new form of carbon. *Nature* **1990**, *347*, 354–358. [[CrossRef](#)]
46. Namin, H.S.; Rahimpour, E.; Ozkan, S.A.; Jouyban, A. An overview on nanostructure-modified supported liquid membranes for the electro membrane extraction method. *Anal. Methods-UK* **2022**, *14*, 212–221. [[CrossRef](#)]
47. Vallant, R.M.; Szabo, Z.; Bachmann, S.; Bakry, R.; Najam-ul-Haq, M.; Rainer, M.; Heigl, N.; Petter, C.; Huck, C.W.; Bonn, G.K. Development and application of C₆₀-fullerene bound silica for solid-phase extraction of biomolecules. *Anal. Chem.* **2007**, *79*, 8144–8153. [[CrossRef](#)]
48. Alheety, M.A.; Raoof, A.; Al-Jibori, S.A.; Karadağ, A.; Khaleel, A.I.; Akbaş, H.; Uzun, O. Eco-friendly C₆₀-SESMP-Fe₃O₄ inorganic magnetizable nanocomposite as high-performance adsorbent for magnetic removal of arsenic from crude oil and water samples. *Mater. Chem. Phys.* **2019**, *231*, 292–300. [[CrossRef](#)]
49. Ghorbani, M.; Seyedin, O.; Aghamohammadhassan, M. Adsorptive removal of lead (II) ion from water and wastewater media using carbon-based nanomaterials as unique sorbents: A review. *J. Environ. Manag.* **2020**, *254*, 109814. [[CrossRef](#)]

50. Journet, C.W.; Maser, W.K.; Bernier, P.; Loiseau, A.; Fischer, J.E. Large-scale production of single-walled carbon nanotubes by the electric-arc technique. *Nature* **1997**, *388*, 756–758. [[CrossRef](#)]
51. Ishigami, M.; Cumings, J.; Zettl, A.; Chen, S. A simple method for the continuous production of carbon nanotubes. *Chem Phys. Lett.* **2000**, *319*, 457–459. [[CrossRef](#)]
52. Hsin, Y.L.; Hwang, K.C.; Chen, F.R.; Kai, J.J. Production and in-situ metal filling of carbon nanotubes in water. *Adv. Mater.* **2001**, *12*, 830–833. [[CrossRef](#)]
53. Zhu, H.W.; Li, X.S.; Jiang, B.; Xu, C.L.; Zhu, Y.F.; Wu, D.H.; Chen, X.H. Formation of carbon nanotubes in water by the electric-arc technique. *Chem. Phys. Lett.* **2002**, *366*, 664–669. [[CrossRef](#)]
54. Vittori Antisari, M.; Marazzi, R.; Krsmanovic, R. Synthesis of multiwall carbon nanotubes by electric arc discharge in liquid environments. *Carbon* **2003**, *41*, 2393–2401. [[CrossRef](#)]
55. Guo, T.; Nikolaev, P.; Thess, A.; Colbert, D.T.; Smalley, R.E. Catalytic growth of single-walled nanotubes by laser vaporization. *Chem. Phys. Lett.* **1996**, *243*, 49–54. [[CrossRef](#)]
56. Rinzler, G.A.; Liu, J.; Dai, H.; Nikolaev, P.; Huffman, B.C. Large-scale purification of single-wall carbon nanotubes: Process, product, and characterization. *Appl. Phys. A* **1998**, *67*, 29–37. [[CrossRef](#)]
57. Nikolaev, P.; Bronikowski, M.J.; Bradley, R.K.; Rohmund, F.; Colbert, D.T.; Smith, K.A.; Smalley, R.E. Gas-phase catalytic growth of single-walled carbon nanotubes from carbon monoxide. *Chem. Phys. Lett.* **1999**, *313*, 91–97. [[CrossRef](#)]
58. Cheng, H.M.; Li, F.; Su, G.; Pan, H.Y.; He, L.L.; Sun, X.; Dresselhaus, G. Large-scale and low-cost synthesis of single-walled carbon nanotubes by the catalytic pyrolysis of hydrocarbons. *Appl. Phys. Lett.* **1998**, *72*, 3282–3284. [[CrossRef](#)]
59. Andrews, R.; Jacques, D.; Rao, A.M.; Derbyshire, F.; Qian, D.; Fan, X.; Dickey, E.C.; Chen, J. Continuous production of aligned carbon nanotubes: A step closer to commercial realization. *Chem. Phys. Lett.* **1999**, *303*, 467–474. [[CrossRef](#)]
60. Feist, B.; Sitko, R. Method for the determination of Pb, Cd, Zn, Mn and Fe in rice samples using carbon nanotubes and cationic complexes of batophenanthroline. *Food Chem.* **2018**, *249*, 38–44. [[CrossRef](#)]
61. Khamirchi, R.; Hosseini-Bandegharai, A.; Alahabadi, A.; Sivamani, S.; Rahmani-Sani, A.; Shahryari, T.; Anastopoulos, I.; Miri, M.; Tran, H.N. Adsorption property of Br-PADAP-impregnated multiwall carbon nanotubes towards uranium and its performance in the selective separation and determination of uranium in different environmental samples. *Ecotox. Environ. Saf.* **2018**, *150*, 136–143. [[CrossRef](#)]
62. Kedziora, K.; Wasiak, W. Extraction media used in needle trap devices-Progress in development and applications. *J. Chromatogr. A* **2017**, *1505*, 1–17. [[CrossRef](#)] [[PubMed](#)]
63. Qian, L.; Shi, J.; Jiang, G. Application of graphene in analytical sample preparation. *TrAC Trend Anal. Chem.* **2012**, *37*, 1–11.
64. Sitko, R.; Zawisza, B.; Malicka, E. Graphene as a new sorbent in analytical chemistry. *TrAC Trend Anal. Chem.* **2013**, *51*, 33–43. [[CrossRef](#)]
65. Wang, J.; Mei, X.; Huang, L.; Zheng, Q.; Qiao, Y.; Zang, K.; Mao, S.; Yang, R.; Zhang, Z.; Gao, Y. Synthesis of layered double hydroxides/graphene oxide nanocomposite as a novel high-temperature CO₂ adsorbent. *J. Energy Chem.* **2015**, *24*, 127–137. [[CrossRef](#)]
66. Zheng, Y.; Cheng, B.; You, W.; Yu, J.; Ho, W.K. 3D hierarchical graphene oxide-NiFe LDH composite with enhanced adsorption affinity to Congo red, methyl orange and Cr (VI) ions. *J. Hazard. Mater.* **2019**, *369*, 214–225. [[CrossRef](#)]
67. Somani, P.R.; Somani, S.P.; Umeno, M. Planer nano-graphenes from camphor by CVD. *Chem. Phys. Lett.* **2006**, *430*, 56–59. [[CrossRef](#)]
68. Arco, L.D.; Yi, Z.; Kumar, A.; Zhou, C. Synthesis, transfer, and devices of single- and few-layer graphene by chemical vapor deposition. *IEEE T Nanotechnol.* **2009**, *8*, 135–138. [[CrossRef](#)]
69. Reina, A.; Jia, X.T.; Ho, J.; Nezich, D.; Son, H.B.; Bulovic, V.; Dresselhaus, M.S.; Kong, J. Large area, few-layer graphene films on arbitrary substrates by chemical Vapor deposition. *Nano Lett.* **2008**, *9*, 30–35. [[CrossRef](#)]
70. Silvestro, I.; Ciarlantini, C.; Francolini, I.; Tomai, P.; Gentili, A.; Dal Bosco, C.; Piozzi, A. Chitosan-graphene oxide composite membranes for solid-phase extraction of pesticides. *Int. J. Mol. Sci.* **2021**, *22*, 8374. [[CrossRef](#)]
71. Sun, W.J.; Hu, X.Y.; Meng, X.Y.; Xiang, Y.H.; Ye, N.S. Molybdenum disulfide-graphene oxide composites as dispersive solid-phase extraction adsorbents for the enrichment of four paraben preservatives in cosmetics. *Microchim. Acta* **2021**, *188*, 256. [[CrossRef](#)]
72. Yan, W.F.; Qiu, S.L. Research progress of porous materials. *Chemistry* **2014**, *77*, 703–708.
73. Zhang, C.H.; Li, G.J.; Wang, J.H. Application of nanopore and porous materials for heavy metal ion detection. *Chin. J. Anal. Chem.* **2014**, *42*, 607–615. [[CrossRef](#)]
74. Zhang, H.F.; Cooper, A.I. Synthesis and applications of emulsion-templated porous materials. *Soft Matter.* **2005**, *1*, 107–113. [[CrossRef](#)] [[PubMed](#)]
75. Rouquerol, F.; Rouquerol, J.; Sing, K.S.W.; Llewellyn, P.; Maurin, G. *Adsorption by Powders and Porous Solids: Principles, Methodology and Applications*; Academic Press: Cambridge, MA, USA, 1999; pp. 163–165.
76. Peng, G.L.; Sharshir, S.W.; Wang, Y.P.; An, M.; Ma, D.K.; Zang, J.F.; Kabeel, A.E.; Yang, N.U. Potential and challenges of improving solar still by micro/nano-particles and porous materials-A review. *J. Clean. Prod.* **2021**, *311*, 127432. [[CrossRef](#)]
77. Suga, M.; Asahina, S.; Sakuda, Y.; Kazumori, H.; Nishiyama, H.; Nokuo, T.; Alfredsson, V.; Kjellman, T.; Stevens, S.M.; Cho, H.S.; et al. Recent progress in scanning electron microscopy for the characterization of fine structural details of nano materials. *Prog. Solid. State. Chem.* **2014**, *42*, 1–21. [[CrossRef](#)]

78. Yaghi, O.M.; Li, G.M.; Li, H.L. Selective binding and removal of guests in a microporous metal-organic framework. *Nature* **1995**, *378*, 703–706. [[CrossRef](#)]
79. Li, X.J.; Ma, W.; Li, H.M.; Zhang, Q.H.; Liu, H.W. Sulfur-functionalized metal-organic frameworks: Synthesis and applications as advanced adsorbents. *Coordin. Chem. Rev.* **2020**, *408*, 213191. [[CrossRef](#)]
80. Wu, Y.L.; Chen, H.L.; Chen, Y.J.; Sun, N.A.R.; Deng, C.H. Metal organic frameworks as advanced extraction adsorbents for separation and analysis in proteomics and environmental research. *Sci. China Chem.* **2022**, *65*, 650–677. [[CrossRef](#)]
81. Morin-Crini, N.; Lichtfouse, E.; Fourmentin, M.; Ribeiro, A.R.L.; Noutsopoulos, C.; Mapelli, F.; Fenyvesi, E.; Vieira, M.G.A.; Picos-Corrales, L.A.; Moreno-Pirajan, J.C.; et al. Removal of emerging contaminants from wastewater using advanced treatments. *Rev. Environ. Chem. Lett.* **2022**, *20*, 1333–1375. [[CrossRef](#)]
82. Khan, N.A.; Hasan, Z.; Jhung, S.H. Adsorptive removal of hazardous materials using metal-organic frameworks (MOFs): A review. *J. Hazard. Mater.* **2013**, *244*, 444–456. [[CrossRef](#)]
83. Barea, E.; Montoro, C.; Navarro, J.A.R. Toxic gas removal–metal-organic frameworks for the capture and degradation of toxic gases and vapours. *Chem. Soc. Rev.* **2014**, *43*, 5419–5430. [[CrossRef](#)] [[PubMed](#)]
84. Ke, F.; Qiu, L.G.; Yuan, Y.P.; Peng, F.M.; Jiang, X.; Xie, A.J.; Shen, Y.H.; Zhu, J.F. Thiol-functionalization of metal-organic framework by a facile coordination-based postsynthetic strategy and enhanced removal of Hg²⁺ from water. *J. Hazard. Mater.* **2011**, *196*, 36–43. [[CrossRef](#)] [[PubMed](#)]
85. Shekhah, O.; Liu, J.; Fischer, R.A.; Woll, C. MOF thin films: Existing and future applications. *Chem. Soc. Rev.* **2011**, *40*, 1081–1106. [[CrossRef](#)]
86. Yaghi, O.M.; O’Keeffe, M.; Ockwig, N.W.; Chae, H.K.; Eddaoudi, M.; Kim, J. Reticular synthesis and the design of new materials. *Nature* **2003**, *423*, 705–714. [[CrossRef](#)] [[PubMed](#)]
87. Ni, Z.; Masel, R.I. Rapid production of metal-organic frameworks via microwave-assisted solvothermal synthesis. *J. Am. Chem. Soc.* **2006**, *128*, 12394–12395. [[CrossRef](#)] [[PubMed](#)]
88. Wu, G.; Ma, J.P.; Wang, S.S.; Chai, H.N.; Guo, L.; Li, J.H.; Ostovan, A.; Guan, Y.F.; Chen, L.X. Cationic metal-organic framework based mixed-matrix membrane for extraction of phenoxy carboxylic acid (PCA) herbicides from water samples followed by UHPLC-MS/MS determination. *J. Hazard. Mater.* **2020**, *394*, 122556. [[CrossRef](#)] [[PubMed](#)]
89. Daliran, S.; Miri, M.G.; Oveisi, A.R.; Khajeh, M.; Navalon, S.; Alvaro, M.; Ghaffari-Moghaddam, M.; Delarami, H.S.; Garcia, H. A pyridyltriazol functionalized zirconium metal-organic framework for selective and highly efficient adsorption of palladium. *ACS Appl. Mater. Interfaces* **2020**, *12*, 25221–25232. [[CrossRef](#)]
90. Amini, S.; Ebrahimzadeh, H.; Seidi, S.; Jalilian, N. Preparation of polyacrylonitrile/Ni-MOF electrospun nanofiber as an efficient fiber coating material for headspace solid-phase microextraction of diazinon and chlorpyrifos followed by CD-IMS analysis. *Food. Chem.* **2021**, *350*, 129242. [[CrossRef](#)]
91. Cote, A.P.; Benin, A.I.; Ockwig, N.W.; O’Keeffe, M.; Matzger, A.J.; Yaghi, O.M. Porous, crystalline, covalent organic frameworks. *Science* **2005**, *310*, 1166–1170. [[CrossRef](#)]
92. El-Kaderi, H.M.; Hunt, J.R.; Mendoza-Cortes, J.L.; Cote, A.P.; Taylor, R.E.; O’Keeffe, M.; Yaghi, O.M. Designed synthesis of 3D covalent organic frameworks. *Science* **2007**, *316*, 268–272. [[CrossRef](#)]
93. Zhao, L.M.; Gan, L.; Zhang, Y. Matrix effect-free on-line pass-through cleanup procedure for the fast determination of local anesthetic drug by LC-MS/MS. *J. Chromatogr. B* **2019**, *1130–1131*, 121831. [[CrossRef](#)] [[PubMed](#)]
94. Wang, R.L.; Li, C.R.; Li, Q.L.; Zhang, S.X.; Lv, F.; Yan, Z.M. Electrospinning fabrication of covalent organic framework composite nanofibers for pipette tip solid phase extraction of tetracycline antibiotics in grass carp and duck. *J. Chromatogr. A* **2020**, *1622*, 461098. [[CrossRef](#)] [[PubMed](#)]
95. Ma, J.B.; Wu, H.W.; Liao, Y.F.; Rui, Q.H.; Zhu, Y.; Zhang, Y. Application of petal-shaped ionic liquids modified covalent organic frameworks for one step cleanup and extraction of general anesthetics in human plasma samples. *Talanta* **2020**, *210*, 120652. [[CrossRef](#)] [[PubMed](#)]
96. Polyakov, M.V.; Khim, Z.F. Adsorption properties and structure of silica gel. *J. Phys. Chem.* **1931**, *2*, 799–805.
97. Fischer, L.; Müller, R.; Ekberg, B.; Mosbach, K. Direct enantioseparation of β -adrenergic blocker using a chiral stationary phase prepared by molecular imprinting. *J. Am. Chem. Soc.* **1991**, *113*, 9358–9360. [[CrossRef](#)]
98. Belbruno, J.J. Molecularly imprinted polymers. *Chem. Rev.* **2019**, *199*, 94–119. [[CrossRef](#)]
99. Kumar, V.; Kim, K.H. Use of molecular imprinted polymers as sensitive/selective luminescent sensing probes for pesticides/herbicides in water and food samples. *Environ. Pollut.* **2022**, *299*, 118824. [[CrossRef](#)]
100. Aylaz, G.; Kuhn, J.; Lau, E.C.H.T.; Yeung, C.C.; Roy, V.A.L.; Duman, M.; Yiu, H.H.P. Recent developments on magnetic molecular imprinted polymers (MMIPs) for sensing, capturing, and monitoring pharmaceutical and agricultural pollutants. *J. Chem. Technol. Biot.* **2021**, *96*, 1151–1160. [[CrossRef](#)]
101. Beyazit, S.; Bui, B.T.S.; Haupt, K.; Gonzato, C. Molecularly imprinted polymer nanomaterials and nanocomposites by controlled/living radical polymerization. *Prog. Polym. Sci.* **2016**, *62*, 1–21. [[CrossRef](#)]
102. Andrade-Eiroa, A.; Canle, M.; Leroy-Cancellieri, V.; Cerda, V. Solid-phase extraction of organic compounds: A critical review (Part I). *TrAC Trends. Anal. Chem.* **2016**, *80*, 641–654. [[CrossRef](#)]
103. Hu, T.L.; Chen, R.; Wang, Q.; He, C.Y.; Liu, S.R. Recent advances and applications of molecularly imprinted polymers in solid-phase extraction for real sample analysis. *J. Sep. Sci.* **2021**, *44*, 274–309. [[CrossRef](#)] [[PubMed](#)]

104. Chen, L.X.; Wang, X.Y.; Lu, W.H.; Wu, X.Q.; Li, J.H. Molecular imprinting: Perspectives and applications. *Chem. Soc. Rev.* **2016**, *45*, 2137–2211. [[CrossRef](#)] [[PubMed](#)]
105. Chen, L.X.; Xu, S.F.; Li, J.H. Recent advances in molecular imprinting technology: Current status, challenges and highlighted applications. *Chem. Soc. Rev.* **2011**, *40*, 2922–2942. [[CrossRef](#)] [[PubMed](#)]
106. Saad, E.M.; El Gohary, N.A.; Abdel-Halim, M.; Handoussa, H.; El Nashar, R.M.; Mizaikoff, B. Molecularly imprinted polymers for selective extraction of rosmarinic acid from *Rosmarinus officinalis* L. *Food Chem.* **2021**, *335*, 127644. [[CrossRef](#)]
107. Li, Z.Z.; Chen, X.J.; Zhang, X.W.; Wang, Y.; Li, D.M.; Gao, H.L.; Duan, X. Selective solid-phase extraction of four phenylarsonic compounds from feeds, edible chicken and pork with tailoring imprinted polymer. *Food Chem.* **2021**, *347*, 129054. [[CrossRef](#)]
108. Abdar, A.; Amiri, A.; Mirzaei, M. Semi-automated solid-phase extraction of polycyclic aromatic hydrocarbons based on stainless steel meshes coated with metal–organic framework/graphene oxide. *Microchem. J.* **2020**, *17*, 107269. [[CrossRef](#)]
109. Feng, J.B.; Li, Y.Y.; Zhang, Y.; Xu, Y.Y.; Cheng, X.W. Adsorptive removal of indomethacin and diclofenac from water by polypyrrole doped-GO/COF-300 nanocomposites. *Chem. Eng. J.* **2022**, *429*, 132499. [[CrossRef](#)]
110. Wu, F.F.; Chen, Q.Y.; Ma, X.J.; Li, T.T.; Wang, L.F.; Hong, J.; Sheng, Y.H.; Ye, M.L.; Zhu, Y. N-doped magnetic covalent organic frameworks for preconcentration of allergenic disperse dyes in textiles of fall protection equipment. *Anal. Methods-UK* **2019**, *11*, 3381–3387. [[CrossRef](#)]
111. Lu, D.K.; Qin, M.H.; Liu, C.; Deng, J.J.; Shi, G.Y.; Zhou, T.S. Ionic liquid-functionalized magnetic metal-organic framework nanocomposites for efficient extraction and sensitive detection of fluoroquinolone antibiotics in environmental water. *ACS. Appl. Mater. Interfaces* **2021**, *13*, 5357–5367. [[CrossRef](#)]
112. Li, F.; Li, X.X.; Su, J.; Li, Y.J.; He, X.W.; Chen, L.X.; Zhang, Y.K. Hydrophilic molecularly imprinted polymers functionalized magnetic carbon nanotubes for selective extraction of cyclic adenosine monophosphate from winter jujube. *J. Sep. Sci.* **2021**, *44*, 2131–2142. [[CrossRef](#)]
113. Cheng, H.L.; Wang, F.L.; Zhao, Y.G.; Zhang, Y.; Jin, M.C.; Zhu, Y. Simultaneous determination of fifteen toxic alkaloids in meat dishes and vegetable dishes using double layer pipette tip magnetic dispersive solid phase extraction followed by UFLC-MS/MS. *Anal. Methods-UK* **2018**, *10*, 1151–1162. [[CrossRef](#)]
114. Lu, Q.; Guo, H.; Zhang, Y.Y.; Tang, X.D.; Lei, W.B.; Qi, R.J.; Chu, J.H.; Li, D.Z.; Zhao, Q.B. Graphene oxide-Fe₃O₄ nanocomposite magnetic solid phase extraction followed by UHPLC-MS/MS for highly sensitive determination of eight psychoactive drugs in urine samples. *Talanta* **2020**, *206*, 120212. [[CrossRef](#)] [[PubMed](#)]
115. Zhao, Y.G.; Li, X.P.; Yao, S.S.; Zhao, P.P.; Liu, J.C.; Xu, C.P.; Lu, Y.Y.; Chen, X.H.; Jin, M.C. Fast throughput determination of 21 allergenic disperse dyes from river water using reusable three-dimensional interconnected magnetic chemically modified graphene oxide followed by liquid chromatography–tandem quadrupole mass spectrometry. *J. Chromatogr. A* **2016**, *1431*, 36–46. [[CrossRef](#)] [[PubMed](#)]
116. Zhao, Y.G.; Zhang, Y.; Wang, F.L.; Zhou, J.; Zhao, Q.M.; Zeng, X.Q.; Hu, M.Q.; Jin, M.C.; Zhu, Y. Determination of perchlorate from tea leaves using quaternary ammonium modified magnetic carboxyl-carbon nanotubes followed by liquid chromatography–tandem quadrupole mass spectrometry. *Talanta* **2018**, *185*, 411–418. [[CrossRef](#)] [[PubMed](#)]
117. Zhang, Y.; Zhao, Y.G.; Chen, W.S.; Cheng, H.L.; Zeng, X.Q.; Zhu, Y. Three-dimensional ionic liquid-ferrite functionalized graphene oxide nanocomposite for pipette-tip solid phase extraction of 16 polycyclic aromatic hydrocarbons in human blood sample. *J. Chromatogr. A* **2018**, *1552*, 1–9. [[CrossRef](#)] [[PubMed](#)]